

Review / Synthèse

A review of polarimetry in the context of synthetic aperture radar: concepts and information extraction

R. Touzi, W.M. Boerner, J.S. Lee, and E. Lueneburg

Abstract. This study provides an update of the polarimetric tools currently being used for optimum information extraction from polarimetric synthetic aperture radar (SAR) images. The basics of polarimetric theory are summarized and discussed in the context of SAR. Calibration of polarimetric SAR, which is an important issue for the extraction of meaningful polarization information, is reviewed. Information extraction using the scattered and received wave parameters and target decomposition theory is considered. In particular, the use of coherent versus incoherent target decomposition is discussed and the practical limitations of these target decompositions are outlined. Speckle filtering and classification of polarimetric SAR images are also thoroughly analyzed, and the important directions for future research are outlined.

Résumé. Cette étude fournit une remise à jour des outils utilisés présentement pour l'extraction de l'information polarimétrique des images radar à ouverture synthétique (ROS). Les bases de la théorie de la polarimétrie sont reconsidérées dans le cadre du ROS. Les méthodes d'étalonnage du ROS polarimétriques sont revues. L'extraction de l'information polarimétrique à partir des paramètres de l'onde diffusée est reconsidérée ainsi que la théorie de la décomposition de cibles. En particulier, l'utilisation de la décomposition cohérente versus la décomposition incohérente est remise en question. Le filtrage du chatoiement et la classification des images polarimétriques sont revus. Les nouvelles orientations de la recherche dans le domaine sont définies.

Introduction

The time-varying direction of the electric field vector, generally describing an ellipse in a plane transverse to propagation, plays an essential role in the interaction of electromagnetic “vector waves” with material bodies and the propagation medium. Whereas this polarization transformation behavior, expressed in terms of the “polarization ellipse”, is named “ellipsometry” in optical sensing and imaging (Azzam, 1977; Born and Wolf, 1959; Jones, 1941; Mueller, 1948; Wolf, 1954), it is denoted “polarimetry” in radar and lidar–ladar sensing and imaging (Boerner et al., 1998; Kennaugh, 1951; Deschamps, 1951; Rumsey, 1951; Graves, 1956; Huynen, 1970; Van Zyl et al., 1987a; Zebker and van Zyl, 1991), using the ancient Greek meaning of “measuring orientation and object shape”. Thus, ellipsometry and polarimetry, which use the basics of the polarization of electromagnetic waves introduced in the 19th century and at the beginning of the 20th century (Stokes, 1852; Wiener, 1930; Mueller, 1948; Born and Wolf, 1959), are concerned with the characterization of the polarization properties of optical and radio waves, respectively. Ellipsometry started a new era in the 1940s with the significant advent of optical polarization phase control devices and the associated development of mathematical ellipsometry, such as the introduction of the 2×2 coherent Jones forward scattering (propagation) matrix (Jones, 1941; 1947) and the associated 4×4 average power density Mueller (Stokes) propagation

matrix (Mueller, 1948). Polarimetry research became active during the late 1940s with the introduction of dual-polarized antenna technology (Kennaugh, 1951; Sinclair, 1950; Rumsey, 1951; Hagfors, 1967; McCormick and Hendry, 1973; 1985) and the subsequent formulation of the 2×2 coherent Sinclair radar backscattering matrix (Sinclair, 1950) and the associated 4×4 Kennaugh radar backscattering power density matrix (Kennaugh, 1951), as summarized in detail in Boerner et al. (1998) and Ulaby and Elachi (1990). Based on the original pioneering work of Kennaugh (1951), Huynen (1965; 1970) developed a phenomenological approach to radar polarimetry that had a subtle impact on the steady advancement of polarimetry (Giuli, 1986) and gave an impetus to further development, which continues today. Since the work of Huynen, important contributions have been made to the

Received 5 November 2003. Accepted 30 January 2004.

R. Touzi.¹ Canada Centre for Remote Sensing, Natural Resources Canada, 588 Booth Street, Ottawa, ON K1A 0Y7, Canada.

W.M. Boerner. Communications and Sensing Laboratory, Department of Electrical Engineering and Computer Science, University of Illinois at Chicago, Chicago, IL 60607-7053, U.S.A.

J.S. Lee. Naval Research Laboratory, Washington, DC 20375, U.S.A.

E. Lueneburg. EML Consultants, Wessling, Germany.

¹Corresponding author (e-mail: Ridha.Touzi@ccrs.nrcan.gc.ca).

application of polarization diversity to improve the detection capability of radar systems (Ionnidis and Hammers, 1979; Poelman and Guy, 1984; Swartz et al., 1988). An excellent contribution was made in the 1980s by Boerner and his coworkers through theoretical studies of the polarization properties of scattering radiation with respect to inverse scattering and target identification (Agrawal and Boerner, 1989; Boerner et al., 1981; 1991; 1993a; 1993b; Boerner and Xi, 1990; Davidovitz and Boerner, 1986; Foo et al., 1984; Kostinski and Boerner, 1986).

In 1985, radar polarimetry started a new era with the National Aeronautics and Space Administration Jet Propulsion Laboratory (NASA-JPL) first imaging airborne radar polarimeter (Van Zyl et al., 1987a; Zebker and Van Zyl, 1991). Whereas early implementations of radar polarimeters utilized conventional techniques with variable physical antenna polarization (Hagfors, 1967; Zebker et al., 1987), the NASA-JPL SAR measured almost simultaneously all the elements of the scattering matrix for each resolution cell. Many sets of data were collected with the NASA CV990 and later with the airborne SAR (AirSAR) (Zebker and Van Zyl, 1991) and were widely distributed and extensively analyzed. Since then, other airborne polarimeters have appeared, such as the ERIM P3 X-, C-, and L-band polarimetric SAR (Kozma et al., 1986); the Canada Centre for Remote Sensing (CCRS) Convair-580 X- and C-band SAR (Livingstone et al., 1989; 1995); the E-SAR S-, L-, and P-band of the German Aerospace Centre (DLR) (Horn et al., 1990; Horn, 1996; Scheiber et al., 1999); the C-band PHARUS SAR (Greidanus et al., 1996); the EMISAR (Skou et al., 1995; Christensen et al., 1998); and more recently the NASDA/CRL L-band Pi-SAR (Wakabayashi et al., 2001) and the ONERA/RAMSES P-, L-, S-, C-, X-, and Ku-band polarimetric SAR (Dubois-Fernandez et al., 2002).² The 10-day shuttle-based mission SIR-C (Freeman et al., 2001; Jordan et al., 1995) in 1994 enabled access to a larger set of polarimetric data, and a wider investigation of the polarimetry in various applications has occurred. Significant contributions to polarization information extraction and sensor calibration techniques appeared during this period and were concretized by special issues of the *IEEE Transactions on Geoscience and Remote Sensing* (IEEE TGRS) and the *International Journal of Remote Sensing* (IGRS) dedicated to calibration (IEEE TGRS, Vol. 30, No. 6, 1992) and polarimetric applications using JPL AirSAR (IJRS, Vol. 15, No. 14, 1994) and SIR-C (IEEE TGRS, Vol. 33, No. 4, 1995) data.

The important well-established literature on the study of partially polarized waves in optics (Born and Wolf, 1959; Jones, 1941; Wolf, 1954; Mandel and Wolf, 1995; Stokes, 1852; Wiener, 1930) serves as the basis for advancing the theory of polarimetry in the context of radar images. Recently, a new impulse to radar polarimetry theory was given by Cloude (1985; 1986) with the introduction of the incoherent target decomposition (ITD). Cloude's ITD, which was shown to be unique (Cloude, 1986) in contrast to Huynen's (1970)

decomposition, provides independent tools derived from the target coherency matrix introduced by Cloude (1986). These tools, which include the Von Neuman entropy H (Von Neumann, 1955; Gamo, 1964; Cloude, 1986), the anisotropy A (Cloude, 1997; Cloude and Pottier, 1997b), and the eigenvector parameters α and β (Cloude and Pottier, 1996; 1997a), were assigned a solid physical interpretation with reference to target scattering mechanisms (Cloude, 1986; Van Zyl, 1992; Cloude and Pottier, 1996; 1997a). Cloude and Pottier's parameters have become the standard tools for target characterization and have been used as the basis for the development of new classification methods introduced for the analysis of polarimetric data (Lee et al., 1999a; Pottier et al., 1999; Ferro-Famil et al., 2001).

As for conventional SAR images, polarimetric SAR images are affected by speckle (Goodman, 1975). The effect of speckle on the polarimetric parameter estimation was first investigated by Goodman in optics (1963; 1975; 1985). Since 1978, the investigation of the effect of speckle on polarimetric parameter statistics has been an active field of research in SAR imagery (Barakat, 1985; Eom and Boerner, 1991; Lee et al., 1994a; Lopes et al., 1992; Murza, 1978; Quegan and Rhodes, 1995; Sarabandi, 1992; Touzi and Lopes, 1991; 1996; Touzi et al., 1999; Vachula and Barnes, 1983). Murza (1978) and Vachula and Barnes (1983) were the first to use the Wishart distribution (Wishart, 1928; Goodman, 1963) to derive the statistics of polarimetric parameters in SAR imagery. Since then, the Wishart distribution has been widely used to assess the effect of multilook speckle on polarimetric tools (Lopes et al., 1992; Lee et al., 1994a; Joughin et al., 1994; Touzi and Lopes, 1996; Touzi et al., 1999) and as the basis of classification and segmentation algorithms (Lee et al., 1994b; 1999a; Ferro-Famil et al., 2001; Beaulieu and Touzi, 2004; Conradsen et al., 2003) and edge-detection techniques (Schou et al., 2003). Speckle filtering of polarimetric SAR images has also been an active area of research for a decade (Novak and Burl, 1990; Lee et al., 1991; Touzi and Lopes, 1994; Lee et al., 1999b; Schou and Skriver, 2001). Touzi and Lopes (1994) were the first to show that a conventional one-channel filter (Lee, 1981; Lee et al., 1994a; Touzi, 2002) cannot preserve the polarimetric information and that speckle filtering should be applied in terms of covariance matrices and not in terms of scattering matrices. Subsequently, various filters that provide a filtered covariance matrices, or the equivalent filtered Mueller, Kennaugh, or target coherency matrix, have been developed (Touzi and Lopes, 1994; Lee et al., 1999b; Lee and Grues, 2000; Schou and Skriver, 2001).

Recently, Cloude and Papathanassiou (1998) and Papathanassiou and Cloude (2001) introduced a technique for optimum information extraction from interferometric-polarimetric (In-Pol) SAR data. The In-Pol SAR technique, which incorporates interferometric height information in SAR polarimetry, looks to be very promising for forest parameter extraction (Treuhaf et al., 1996; Treuhaf and Siqueira, 2000;

²A review of polarimetric airborne and satellite SAR systems and their parameters can be found in Raney (1998).

Papathanassiou and Cloude, 2003). Unfortunately, the state of the art in In-Pol SAR techniques and applications is not discussed in this paper, which focuses on information extraction from one-pass polarimetric SAR.

Polarimetry, which has been an active area of research for about 50 years, has been thoroughly summarized in various books and review papers (Azzam, 1977; Born and Wolf, 1959; Chandrasekhar, 1960; Giuli, 1986; Kennaugh, 1951; Mott, 1992; Tsang et al., 1985; Kong, 1990; Van Zyl and Zebker, 1990; Zebker and Van Zyl, 1991; Ulaby and Elachi, 1990). An excellent review has recently been completed by Boerner et al. (1998). With all the upcoming satellite polarimetric SARs, such as RADARSAT-2 (Luscombe et al., 2000), ALOS-PALSAR (Ito et al., 2001), and TerraSAR X- and L-bands (Schwerdt et al., 2003; Mathew, 2001), it is important to provide an update of the polarimetric tools currently being used for polarimetric information extraction. In this study, the most well known tools are thoroughly considered and analyzed in the context of SAR, and the important directions for future research are outlined. The basis of the polarimetric theory is summarized. Characterization of quasi-monochromatic and partially polarized waves is discussed in the context of SAR imagery. Calibration of polarimetric SAR, which is an important issue for the extraction of meaningful polarization information, is reviewed. The various methods are presented for target characterization using the polarization information of target scattered and received waves. Coherent and incoherent target decomposition techniques, the various polarimetric speckle filters, and the various classification methods developed for polarimetric SAR imagery are reviewed. Their limitations are discussed as a function of speckle and scene characteristics.

Polarization of monochromatic electromagnetic plane waves

Ellipse mathematical equation

The polarization of a monochromatic electromagnetic plane wave describes the shape and locus of the electric vector end point in a plane orthogonal to the direction of wave propagation (Born and Wolf, 1959; Chandrasekhar, 1960). Let $\vec{r}(x, y, z)$ be a position vector of a point P in space illuminated by the wave characterized by the wave vector \vec{k} . The electromagnetic wave is fully characterized by the parameters (magnitude, phase, and direction) of its electric vector $\vec{E}(\vec{r}, t)$ given by

$$\vec{E}(\vec{r}, t) = E_x \vec{x} + E_y \vec{y} \tag{1}$$

$$= [a_x \cdot \exp(j\delta_x) \vec{x} + a_y \cdot \exp(j\delta_y) \vec{y}] \cdot \exp[j(\omega t - kz)]$$

where ω is the angular frequency; and δ_x and δ_y are the x and y phases, respectively, of the (\vec{E}) components (Born and Wolf, 1959; Boerner et al., 1981). The corresponding Cartesian components E_1 and E_2 of the real vector $\text{Real}(\vec{E})$ are

$$E_1 = a_x \cos(\tau + \delta_x)$$

$$E_2 = a_y \cos(\tau + \delta_y) \tag{2}$$

where $\tau = \omega t - kz$. Elimination of the time-varying parameter τ between the two expressions in Equation (2) leads to the equation of the curve described by the end point of the electric field in the plane (x, y):

$$\frac{E_1^2}{a_x^2} + \frac{E_2^2}{a_y^2} - 2 \frac{E_1 E_2}{a_x a_y} \cos \delta = \sin^2 \delta \tag{3}$$

where $\delta = \delta_y - \delta_x$ is the phase difference between the \vec{x} and \vec{y} components (Born and Wolf, 1959). For a monochromatic wave, a_x , a_y , and δ are constant (do not depend on time), and Equation (3) corresponds to an ellipse. When the phase difference δ is zero or a multiple number of π , the ellipse reduces to a straight line and the wave is said to be linearly polarized. When the two components are of the same magnitude ($a_x = a_y$) and are in quadrature of phase ($\delta = \pm\pi/2$), the ellipse reduces to a circle and the wave is said to be circularly polarized (Born and Wolf, 1959).

Polarization state characterization

Jones vector

Figure 1 represents the ellipse of Equation (3) described in the wave plane (\vec{x}, \vec{y}). The polarization ellipse might be characterized using the three independent quantities a_x , a_y , and δ or the three equivalent independent entities $s_0 = a_x^2 + a_y^2$, $\alpha = \arctan(a_y/a_x)$, and δ . It might also be characterized by the major and minor axes a_ξ and a_η and the angle ψ ($0 \leq \psi \leq \pi$), which specifies the orientation of the ellipse, or the three equivalent independent entities $s_0 = a_\xi^2 + a_\eta^2 = a_x^2 + a_y^2$, the ellipticity angle $\chi = \arctan(a_\eta/a_\xi)$ ($-\pi/4 \leq \chi \leq \pi/4$), and the orientation angle ψ . The ellipse angles ψ and χ are related to the polarization ellipse angles α and δ by (Deschamps, 1951; Born and Wolf, 1959).

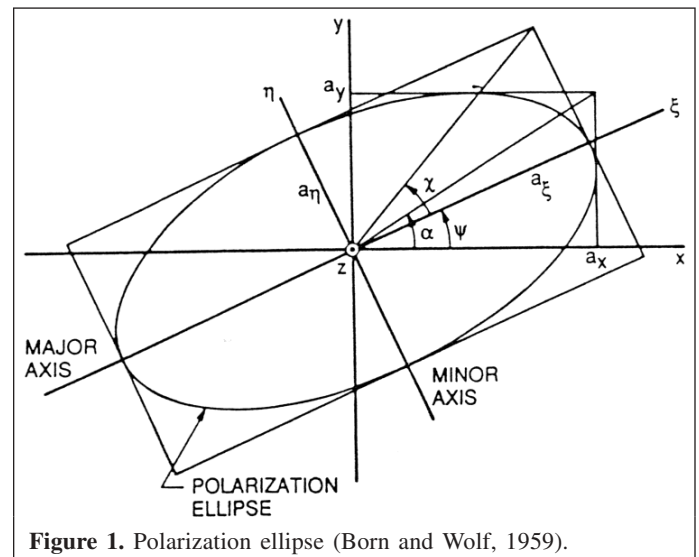


Figure 1. Polarization ellipse (Born and Wolf, 1959).

$$\tan 2\psi = (\tan 2\alpha)\cos \delta$$

$$\sin 2\chi = \sin 2\alpha \sin \delta \tag{4}$$

The polarization of the wave of Equation (1) is defined by the Jones vector (Jones, 1941; Born and Wolf, 1959; Boerner et al., 1981), which is derived from Equation (1) after removal of the time harmonic component $\exp[j(\omega t - kz)]$ and the absolute phase δ_x as

$$\vec{h}(\alpha, \delta) = [\cos \alpha \vec{x} + \sin \alpha \exp(j\delta)\vec{y}] \cdot \|\vec{E}\| = \vec{P}_s \cdot \|\vec{E}\| \tag{5}$$

where δ is the channel phase difference, and $\|\vec{E}\|^2 = s_0$ is the total intensity. Usually, the normalized Jones vector $\vec{P}_s = \vec{h} / \|\vec{E}\|$ is used to represent the so-called polarization state. This vector might also be presented as a function of the ellipse angles (ψ, χ) :

$$\vec{P}_s(\psi, \chi) = [\mathbf{Rot}(\psi)](\cos \chi \cdot \vec{x} + j \sin \chi \cdot \vec{y}) \tag{6}$$

where $[\mathbf{Rot}(\psi)]$ is the matrix of the rotation ψ to be applied to transform the ellipse basis (\vec{x}, \vec{y}) to the basis (\vec{x}, \vec{y}) (Kennaugh, 1951; Huynen, 1970).

Stokes vector

It was as early as 1852 when Stokes showed that a nearly monochromatic plane light wave may be characterized by four real and observable parameters that now bear his name (Stokes, 1852; Wolf, 1954; Van de Hulst, 1957; Born and Wolf, 1959):

$$\begin{aligned} \vec{S}^T &= [s_0, s_1, s_2, s_3]^T \\ &= [a_x^2 + a_y^2, a_x^2 - a_y^2, 2a_x a_y \cos \delta, 2a_x a_y \sin \delta]^T \\ &= s_0 [1, \cos 2\chi \cos 2\psi, \cos 2\chi \sin 2\psi, \sin 2\chi]^T \end{aligned} \tag{7}$$

The three independent parameters of the polarization ellipse (a_x, a_y, δ) are now represented using the four Stokes parameters $s_0, s_1, s_2,$ and s_3 , which correspond to three independent quantities, since

$$s_0^2 = s_1^2 + s_2^2 + s_3^2 \tag{8}$$

(Jones, 1947; Deschamps, 1951; Schneider, 1969). Notice that the absolute phase δ_x is not preserved in the Stokes representation.

The Stokes parameters were the first means proposed to describe polarization in terms of directly observable (power) quantities (Wolf, 1954; Born and Wolf, 1959; Parrent and Roman, 1960). Using the Stokes representation, the state of polarization can be uniquely mapped to a point P of Cartesian coordinates (s_1, s_2, s_3) on a sphere of radius s_0 (the electric field intensity) named the Poincaré sphere (Poincaré, 1892). The concept of representing wave polarization state as a point on a sphere, which was originally set by Poincaré to describe the polarization state of the light, was adapted to radio waves and antennas by Deschamps (1951) and shown to be convenient for

representing and solving polarization problems such as adaptation of transmitting–receiving antenna polarizations (Deschamps, 1951; Deschamps and Mast, 1973; Poelman and Guy, 1984). The normalized polarization state corresponding to an ellipse of angles (ψ, χ) can be mapped as a point on the unit radius Poincaré sphere of latitude 2χ and longitude 2ψ , as seen in **Figure 2**. Because the sign of χ determines the handedness of the polarization state, the upper hemisphere (corresponding to $\chi > 0$) displays left-handed polarizations and the lower hemisphere displays right-handed polarizations, according to the Institute of Electrical and Electronics Engineers standard definitions of terms for antennas (IEEE, 1983). The poles represent the circular polarizations, whereas linear polarizations are represented by points in the equatorial plane (Deschamps, 1951; Van Zyl and Zebker, 1990).

Characterization of partially coherent plane waves

Quasi-monochromatic and partially polarized waves

With SAR, wave transmission is narrow-band (Raney, 1980; Curlander and McDonough, 1991), and transmitted and received waves are narrow-band about the central mean frequency $\bar{\omega}$:

$$\bar{\omega} - \frac{1}{2} \Delta\omega \leq \omega \leq \bar{\omega} + \frac{1}{2} \Delta\omega \quad \text{with} \quad \frac{\Delta\bar{\omega}}{\bar{\omega}} \ll 1 \tag{9}$$

In this case, the wave, which may still be interpreted as a plane wave, is said to be quasi-monochromatic, and the components E_1 and E_2 of the real vector $\text{Real}[\vec{E}]$ at each point are given by

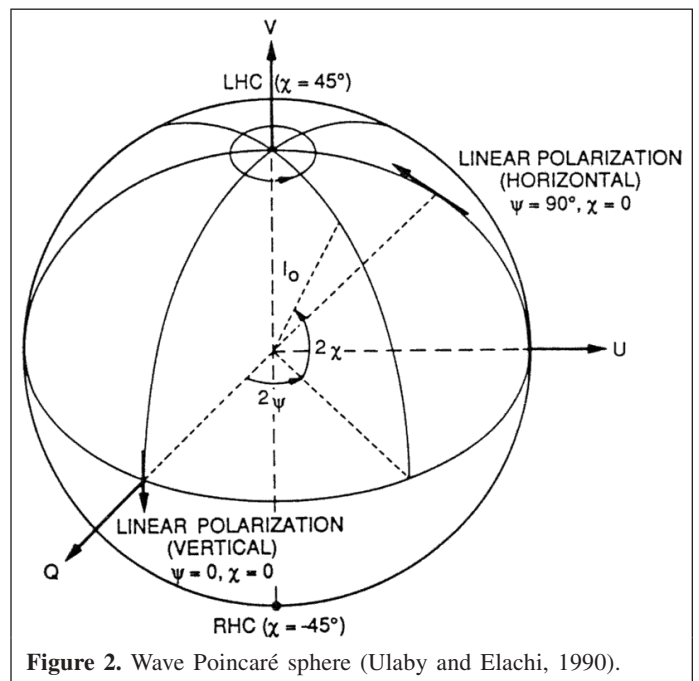


Figure 2. Wave Poincaré sphere (Ulaby and Elachi, 1990).

$$\begin{aligned} E_1(P, t) &= a_x(t) \cos[\bar{\omega}t - \bar{k}z + \delta_x(t)] \\ E_2(P, t) &= a_y(t) \cos[\bar{\omega}t - \bar{k}z + \delta_y(t)] \end{aligned} \quad (10)$$

where $\bar{\omega}$ denotes the mean frequency; \bar{k} is the mean wave vector; and $a_x(t)$, $a_y(t)$, $\delta_x(t)$, and $\delta_y(t)$ are slowly varying in comparison with the periodic term $\exp[j(\bar{\omega}t)]$ (Born and Wolf, 1959; Barakat, 1985). The receiving antenna measures the target scattered narrow-band wave during an interval of time T , named the azimuth integration time. If this time measurement is small compared with the target coherence time (Born and Wolf, 1959; Raney, 1980), the ellipse quantities $a_x(t)$, $a_y(t)$, $\delta_x(t)$, and $\delta_y(t)$ can be assumed to be constant, and the wave behaves in the time interval T like a monochromatic wave with mean frequency $\bar{\omega}$ (Born and Wolf, 1959). Either the Jones vector or the Stokes vector can then be used to characterize the polarization of the wave that is said to be a completely polarized wave. For a longer time interval, however, the aforementioned parameters are time varying and the wave is said to be partially polarized (Born and Wolf, 1959; Van Zyl et al., 1987b; Kostinsky and Boerner, 1986). In this case, the parameters that characterize the polarization wave should be time averaged and are only meaningful under signal wide-sense stationarity and ergodicity conditions. The information provided by the time electric field components correlation was shown to be necessary for the characterization of partially polarized waves, and the coherency matrix has to be measured instead of the electric field for the characterization of partially polarized waves (Wiener, 1930; Wolf, 1954; 1959; Born and Wolf, 1959; Kim et al., 1987).

Coherency matrix for the representation of partially polarized waves

The coherency matrix is an interesting tool that permits observable parameters of a partially polarized wave to be measured (Wolf, 1959; Parrent and Roman, 1960). With quasi-monochromatic waves the rapid oscillations $\exp(j\bar{\omega}t)$ cancel out, and the electric field complex signal is intimately connected with the envelop-like variations (Born and Wolf, 1959; Barakat, 1985; Kostinski and Boerner, 1986). Electric fields parameters should be time averaged, under the assumption of signal stationary and ergodicity, to end up with measurable quantities that can characterize wave polarization. To deal with observable quantities, two quadratic forms of the quadratic products of \vec{E} and \vec{E}^{*T} are considered (Jones, 1947; Wolf, 1959; Parrent and Roman, 1960; Schneider, 1969): the time-averaged total intensity $\langle \vec{E}^{*T} \cdot \vec{E} \rangle$, and the coherency (2×2) Hermitian matrix (Wiener, 1930; Wolf, 1954; Born and Wolf, 1959):

$$[\mathbf{J}] = \langle \vec{E} \cdot \vec{E}^{*T} \rangle \quad (11)$$

The sharp brackets $\langle \dots \rangle$ indicate ensemble averaging and can be replaced by time averaging if ergodicity can be assumed, and $[\mathbf{J}]$ is Hermitian positive semi-definite (i.e., it has non-negative eigenvalues). The fact that $[\mathbf{J}] = [\mathbf{J}]^{*T}$ makes $[\mathbf{J}]$ an

observable quantity, and in practice the time average of $[\mathbf{J}]$ is measurable. The trace s_0 of the matrix $[\mathbf{J}]$ is the total intensity of the wave (Born and Wolf, 1959):

$$s_0 = \|\vec{E}\|^2 = \text{Tr}[\mathbf{J}] \quad (12)$$

The coherency matrix $[\mathbf{J}]$, also named the correlation tensor, was originally introduced by Wiener (1930) and Wolf (1954) for the description of partially polarized waves of stationarity electromagnetic field. This matrix is equivalent to the density matrix of Von Neuman that was widely used in quantum mechanics (Wolf, 1954). Wolf has shown (Wolf, 1959; Born and Wolf, 1959) that the four elements of the coherency matrix $[\mathbf{J}]$ are uniquely associated with the wave and that the unique set obtained is intimately related to the appropriate degree of coherence of the electric fields in the two orthogonal directions:

$$[\mathbf{J}] = \begin{bmatrix} J_{xx} & J_{xy} \\ J_{yx} & J_{yy} \end{bmatrix} = \begin{bmatrix} \langle |E_x|^2 \rangle & \langle E_x E_y^* \rangle \\ \langle E_y E_x^* \rangle & \langle |E_y|^2 \rangle \end{bmatrix} \quad (13)$$

$$= \begin{bmatrix} \langle |a_x|^2 \rangle & \langle a_x a_y \exp(-j\delta) \rangle \\ \langle a_x a_y \exp(j\delta) \rangle & \langle |a_y|^2 \rangle \end{bmatrix}$$

If the x and y axes are rotated about the direction of propagation, the coherency matrix changes. However, the determinant $|\mathbf{J}|$ of $[\mathbf{J}]$, the two real non-negative eigenvalues λ_1 and λ_2 , and the trace of the Hermitian coherency matrix $[\mathbf{J}]$ remain rotation invariant. Combination of these entities leads to a rotation-invariant parameter, the degree of polarization of the wave given by (Wolf, 1959; Born and Wolf, 1959)

$$p = \sqrt{1 - \frac{4|\mathbf{J}|}{\text{Tr}(\mathbf{J})^2}} = \frac{|\lambda_2 - \lambda_1|}{\lambda_2 + \lambda_1} \quad (14)$$

The $[\mathbf{J}]$ eigenvalues, λ_2 and λ_1 , correspond to the extrema of the total intensity (Wolf, 1959; Born and Wolf, 1959). The rotation-invariant parameter, p , has a physical significance (Born and Wolf, 1959); it corresponds to the ratio of the completely polarized wave to the total wave intensity. The wave is considered to be completely polarized if $|\mathbf{J}| = 0$; this corresponds to $p = 1$. The wave is said to be completely unpolarized if the intensity of its components in any direction perpendicular to the direction of propagation is a constant. In this case, the coherence matrix is diagonal, and the two elements of the diagonal are identical, leading as such to $p = 0$.

Stokes vector for representation of partially polarized waves

A partially polarized wave can also be characterized by the four time-averaged Stokes parameters of Equation (7), since they are simply related to the elements of the coherency matrix by

$$\begin{aligned}
s_0 &= J_{xx} + J_{yy} = \langle |a_x|^2 \rangle + \langle |a_y|^2 \rangle \\
s_1 &= J_{xx} - J_{yy} = \langle |a_x|^2 \rangle - \langle |a_y|^2 \rangle \\
s_2 &= J_{xy} + J_{yx} = 2\langle a_x a_y \cos(\delta) \rangle \\
s_3 &= j(J_{xy} - J_{yx}) = 2\langle a_x a_y \sin(\delta) \rangle
\end{aligned} \tag{15}$$

The one-to-one correspondence between the coherency matrix and the Stokes vector allowed Wolf (1959) to extend to the Stokes parameters the results he obtained regarding the uniqueness of the coherency matrix associated with a wave, and a unique set of Stokes parameters was shown to characterize a partially polarized wave.

The non-negative condition satisfied for the determinant of the coherency matrix $[\mathbf{J}]$ expressed in term of the Stokes parameters implies (Wolf, 1959; Born and Wolf, 1959),

$$s_0^2 \geq s_1^2 + s_2^2 + s_3^2 \tag{16}$$

and the degree of polarization of Equation (14) is given by

$$p = \frac{\sqrt{s_1^2 + s_2^2 + s_3^2}}{s_0} \tag{17}$$

The degree of polarization was qualified as the most important parameter associated with the state of partial polarization of optic waves (Jones, 1947; Wolf, 1959; Mandel, 1963). This tool has been successfully applied for target scattering characterization (Poelman and Guy, 1984; Touzi et al., 1992a), as discussed in the following.

Mathematical characterization of target scattering

Scattering matrix

The scatterer illuminated by the SAR transmitted wave re-radiates a scattered wave, which might be considered as a spherical wave in the far zone of the scatterer. This wave can be approximated by a plane wave over the relatively small area occupied by the receiving antenna. The electric fields \vec{E}^s and \vec{E}^i of the scattered wave and the incident waves are related by the complex 2×2 scattering matrix $[\mathbf{S}]$ of the scatterer defined according to

$$\vec{E}^s = \frac{\exp(jkr)}{r} \cdot [\mathbf{S}] \cdot \vec{E}^i \tag{18}$$

where r is the distance between the target and the antenna (Jones, 1941; Sinclair, 1950; Kennaugh, 1951; Kostinski and Boerner, 1986; Van Zyl and Zebker, 1990). Here the backscattered alignment (BSA)³ convention, which has been the preferred system in the area of monostatic SAR polarimetry

(Van Zyl and Zebker, 1990), is used and the scattering matrix defined in Equation (18) relates the scattered wave viewed approaching the receiving antenna to the incident wave viewed receding from the transmitting antenna (Van Zyl et al., 1987a). The $[\mathbf{S}]$ matrix, which is expressed in the BSA coordinates, is referred to as the Sinclair matrix (Sinclair, 1950; Kennaugh, 1952; Zebker and Van Zyl, 1991; Guissard, 1994; Boerner et al., 1998) and is given in the horizontal-vertical polarization basis (h, v) per

$$[\mathbf{S}] = \begin{bmatrix} S_{hh} & S_{hv} \\ S_{vh} & S_{vv} \end{bmatrix} \tag{19}$$

where S_{hv} denotes a transmitting antenna of a horizontal polarization and a receiving antenna of a vertical polarization (Van Zyl et al., 1987a; Zebker and Van Zyl, 1991; Boerner et al., 1998). $[\mathbf{S}]$ becomes symmetric if the target is reciprocal, $S_{hv} = S_{vh}$.

Power backscattering matrix: Graves matrix

The total power P_s backscattered from the target for any transmitted polarization is the magnitude squared of the scattered wave electric field \vec{E}^s and can be expressed as a function of the transmitted wave electric field \vec{E}^i using Equation (18):

$$P_s = \frac{1}{r^2} (\vec{E}^i)^{*T} \cdot [\mathbf{G}] \cdot \vec{E}^i \tag{20}$$

where the Hermitian positive semi-definite matrix $[\mathbf{G}]$, which is referred to as the Graves matrix (Graves, 1956) or the "polarization power scattering matrix" (Graves, 1956; Boerner et al., 1998), is given by

$$[\mathbf{G}] = [\mathbf{S}]^{*T} [\mathbf{S}] \tag{21}$$

Mueller and Kennaugh matrices

Using the BSA convention, the Stokes vector of the backscattered wave is related to the incident-wave Stokes vector through the Kennaugh matrix, $[\mathbf{K}]$ (Kennaugh, 1951; Van de Hulst, 1957; Van Zyl et al., 1987a; Boerner et al., 1998):

$$\vec{S}^s = \frac{1}{r^2} \cdot [\mathbf{K}] \cdot \vec{S}^i \tag{22}$$

Here, the BSA convention is used and the 4×4 Kennaugh matrix $[\mathbf{K}]$ is given by (Guissard, 1994; Boerner et al., 1998)

$$[\mathbf{K}] = 2[\mathbf{A}]^* \cdot [\mathbf{W}] \cdot [\mathbf{A}]^{-1} \tag{23}$$

with

³Reviews of the two major conventions currently used for coordinates systems, the forward-scatter alignment (FSA) convention and the BSA convention, can be found in Van Zyl and Zebker (1990), Guissard (1994), and Boerner et al. (1998).

$$[\mathbf{W}] = [\mathbf{S}] \otimes [\mathbf{S}]^* \quad (24)$$

where \otimes symbolizes the standard tensorial Kronecker matrix product, and the 4×4 expansion matrix $[\mathbf{A}]$ is given by

$$[\mathbf{A}] = \begin{bmatrix} 1 & 0 & 0 & 1 \\ 1 & 0 & 0 & -1 \\ 0 & 1 & 1 & 0 \\ 0 & j & -j & 0 \end{bmatrix} \quad (25)$$

with $A^{-1} = (1/2)A^{*T}$ (Guissard, 1994; Boerner et al., 1998).

In optical or transmission polarimetry, the FSA convention is used and the Stokes vector of the scattered wave is related to the incident-wave Stokes vector through the Mueller matrix $[\mathbf{M}]$ (Mueller, 1948; Chandrasekhar, 1960; Tsang et al., 1985; Kong, 1990):

$$\vec{S}^s = \frac{1}{r^2} \cdot [\mathbf{M}] \cdot \vec{S}^i \quad (26)$$

The Mueller matrix $[\mathbf{M}]$ and the Kennaugh matrix $[\mathbf{K}]$ are formally related by (Guissard, 1994; Lüneburg, 1995a; Boerner et al., 1998)

$$[\mathbf{M}] = \text{diag}[1 \ 1 \ 1 \ -1] \cdot [\mathbf{K}] \quad (27)$$

This relation is only formally correct, since both matrices describe completely different scattering mechanisms: forward scattering for $[\mathbf{M}]$ and backscattering for $[\mathbf{K}]$. Multilook SAR data are generally provided under the Kennaugh matrix format and the system reciprocity assumption (Dubois and Norikane, 1987).

Scattering or Mueller–Kennaugh matrix for wave characterization

If the illuminated target re-radiates a completely polarized scattered wave, the polarization of the wave can be deduced from the polarization of the transmitting antenna using either the scattering matrix $[\mathbf{S}]$ or the Mueller–Kennaugh matrix. Generally, there are seven independent parameters in the scattering matrix: four independent amplitudes and three phases referenced to one element of the four $[\mathbf{S}]$ complex elements. Therefore, if the absolute reference phase is ignored, only seven real elements should completely characterize $[\mathbf{M}]$ or $[\mathbf{K}]$, and as a result there are nine relations among the 16 elements of the matrix (Simon, 1982; Barakat, 1981; Giuli, 1986; Van Zyl et al., 1987a). Under the reciprocity assumption, $S_{hv} = S_{vh}$ and $[\mathbf{S}]$, $[\mathbf{K}]$, and $[\mathbf{M}]$ are characterized by only five real elements.

Partially polarized waves cannot be characterized by the scattering matrix, and the description of the SAR–target system in terms of $[\mathbf{M}]$ or $[\mathbf{K}]$ appears to be applicable to more general

situations than the description in terms of the scattering matrix (Wolf, 1959; Born and Wolf, 1959). Howell (1979) has shown that some optical devices can be described by the Mueller matrix but not by the scattering matrix. Other studies have confirmed this result (Azzam, 1977; Kim et al., 1987). Sixteen real elements are needed to fully characterize the system in the general case, and nine elements are needed under the reciprocity assumption (Kostinski and Boerner, 1986; Van Zyl et al., 1987a).

In addition to $[\mathbf{M}]$ and $[\mathbf{K}]$, two matrices named the target covariance matrix and the target coherence matrix might be used for characterization of partially polarized waves. These matrices are presented in the following section.

Target covariance and target coherency matrices

The scattering matrix of Equation (18) can be represented under the vectorial form

$$\vec{S} = (S_{hh}, S_{hv}, S_{vh}, S_{vv})^T \quad (28)$$

An ensemble average of the complex product between \vec{S} and \vec{S}^{*T} leads to the so-called covariance matrix⁴ $[\mathbf{C}]$ (Borgeaud et al., 1987; Van Zyl and Ulaby, 1990):

$$[\mathbf{C}] = \langle \vec{S} \cdot \vec{S}^{*T} \rangle \quad (29)$$

The Hermitian positive semi-definite matrix $[\mathbf{C}]$ has precisely the same elements as the Kennaugh matrix $[\mathbf{K}]$ and the Mueller matrix $[\mathbf{M}]$ but with different arrangements. The full established properties of Hermitian matrices make convenient the use of $[\mathbf{C}]$ in some applications (Borgeaud et al., 1987; Kong et al., 1987; Novak and Burl, 1990; Van Zyl, 1992; Touzi and Lopes, 1994).

Another matrix that contains the same information as the Mueller matrix is the target coherency matrix $[\mathbf{T}]$, which was introduced by Cloude (1986) and used for the development of his incoherent target decomposition (Cloude and Pottier, 1996; 1997a). The target coherency matrix, which was defined per analogy with the wave coherency matrix, is given by (Cloude, 1986; Cloude and Pottier, 1996)

$$[\mathbf{T}] = \langle \vec{k} \cdot \vec{k}^{*T} \rangle \quad (30)$$

where \vec{k} is the target scattering vector (Cloude, 1986) and is given by

$$\vec{k} = [S_{hh} + S_{vv}, S_{hh} - S_{vv}, S_{hv} + S_{vh}, j(S_{hv} - S_{vh})]^T \quad (31)$$

Note that Equation (31) might be written under the vectorial form as

$$\vec{k} = [\mathbf{A}] \cdot \vec{S} \quad (32)$$

⁴Even though $[\mathbf{C}]$ corresponds to the covariance matrix for a zero mean process like speckle, the term covariance matrix is adopted (instead of correlation matrix) for the more general case of nonzero mean process (Tragl, 1990; Van Zyl and Ulaby, 1990).

It is worth noting that $[C]$ and $[T]$ are unitarily similar (up to a constant), as might be shown using Equation (32). The two matrices carry the same information; both are Hermitian positive semi-definite and both have the same eigenvalues but different eigenvectors (Cloude and Pottier, 1996).

Polarization synthesis and received intensity

The power received from the illuminated resolution cell might be expressed as a function of the Jones vectors \vec{p}^t and \vec{p}^r of the transmitting and receiving antenna by (Kostinski and Boerner, 1986; Van Zyl et al., 1987a; Ulaby and Elachi, 1990; Boerner et al., 1998)

$$P_{\text{rec}}(\Psi_r, \chi_r, \Psi_t, \chi_t) = \frac{\mathcal{L}}{r^2} \cdot |\vec{p}^r \cdot [S] \vec{p}^t|^2 \quad (33)$$

where \mathcal{L} is a constant depending on the system losses, peak transmitter power, length of the transmitted pulse, number of samples integrated in range, antenna beamwidth, SAR velocity, transmitted wavelength, permittivity and permeability of free space, and antenna gain at the target illumination angle θ (Touzi et al., 1993). The radar equation (Equation (33)) and the voltage equation (Equation (18)) are referred to as the fundamental equations of radar polarimetry (Kostinski and Boerner, 1986; Van Zyl and Zebker, 1990). The received radar backscattering can be synthesized for any combination of transmitting–receiving antennas (see, for example, in Van Zyl et al., 1987a the various images of San Francisco Bay synthesized for transmitting and receiving antennas of the same polarization with the ellipse angles sampled at 2.5°).

Multilook SAR data are generally provided under the Kennaugh matrix format (Dubois and Norikane, 1987). In this case, the received power can be synthesized for any combination of transmitting–receiving polarizations expressed in terms of Stokes vectors \vec{S}^t and \vec{S}^r as (Van Zyl and Zebker, 1990; Boerner et al., 1998)

$$P_{\text{rec}}(\Psi_r, \chi_r, \Psi_t, \chi_t) = \frac{\mathcal{L}}{r^2} \cdot |\vec{S}^r \cdot [K] \cdot \vec{S}^t| \quad (34)$$

Generally, the received power is averaged over many pixels, say N , for estimation of the target received power mean. To preserve the full polarization information, the averaging should be conducted under the Kennaugh matrix format:

$$\hat{P}_{\text{rec}}(\Psi_r, \chi_r, \Psi_t, \chi_t) = \frac{\mathcal{L}}{Nr^2} \cdot \vec{S}^r \cdot \sum_{n=1}^N [K]_n \cdot \vec{S}^t \quad (35)$$

where $[K]_n$ is the Kennaugh matrix of the pixel n (Van Zyl et al., 1987a; Dubois and Norikane, 1987; Zebker and Van Zyl, 1991; Boerner et al., 1998). If the data are provided in $[S]$ matrix, each pixel $[S]$ matrix should be transformed in $[K]$ matrix, and the integration is completed in terms of Kennaugh matrices using Equation (35).

Even though the data are generally provided in $[S]$ or $[K]$ matrix format, it might be convenient for some applications to express the received power as a function of the covariance matrix $[C]$ of Equation (29) (see, for example, Swartz et al., 1988; and Touzi and Lopes, 1994). For an antenna operating at the horizontal–vertical polarization basis, the received power is given by (Swartz et al., 1988; Van Zyl and Zebker, 1990; Mattia et al., 1997)

$$P_{\text{rec}}(\Psi_r, \chi_r, \Psi_t, \chi_t) = \frac{\mathcal{L}}{r^2} \cdot |\vec{B}^{*T} \cdot [C] \cdot \vec{B}| \quad (36)$$

where \vec{B} is a mixed antenna vector given, as a function of \vec{p}^r coordinates (p_h^r, p_v^r) and \vec{p}^t coordinates (p_h^t, p_v^t) , by

$$\vec{B}^{*T} = (p_h^r p_h^t, p_h^r p_v^t, p_v^r p_h^t, p_v^r p_v^t) \quad (37)$$

Calibration of polarimetric SAR data: an important issue for the extraction of meaningful polarization information

An imaging polarimeter is usually implemented by configuring the hardware to measure almost simultaneously the four scattering matrix elements for every resolution element in the scene (Christensen et al., 1998; Livingstone et al., 1995; Van Zyl et al., 1987a; Zebker and Van Zyl, 1991). All existing imaging polarimeters provide the four measurements in the linear horizontal (H) and vertical (V) polarizations HH, HV, VH, and VV. These measurements might be affected by crosstalk due to the transmitting–receiving antenna or the switches used to select the H or V polarization at transmission and reception (Touzi et al., 1993). Since 1989, intense attention has been given to the importance of calibration for the meaningful use of polarimetric data. Van Zyl (1990) was the first to introduce a method for the calibration of the AirSAR data using image parameters and reference point targets. Since then, many papers have been published on the calibration of polarimetric AirSAR data, which were widely diffused and extensively used all over the world (Freeman, 1991; 1992; Freeman et al., 1992; Klein, 1992; Quegan, 1993; Zebker and Lou, 1990; Touzi et al., 1993). The appearance of other polarimetric SARs has led to the development of various specific system calibration methods (Christensen et al., 1998; Horn, 1996; Skriver et al., 1994; Touzi et al., 1993). In parallel with the calibration and flying the AirSAR system in the 1990s, there was an important ongoing JPL activity (led by A. Freeman) that was focused on the preparation and calibration of the first satellite polarimetric SAR mission, SIR-C, realized by the shuttle *Discovery* in 1994 (Jordan et al., 1995; Freeman, 1995; Dubois, 1992).

To calibrate a polarimetric SAR system, accurate system modeling should be completed. Most of the calibration methods were based on the Barnes model developed in 1986 (Barnes, 1986). A more general model, which explicitly separates the antenna distortion from other key radar

architecture elements, was introduced by Touzi et al. (1993). This model is suitable for most existing systems that use only one configuration at reception and for systems with two receiving configurations (dependent on the transmitted polarization) like the Convair-580 SAR system (Livingstone et al., 1995). The voltage matrix $[\mathbf{V}]$ received by a SAR system (with one receiving configuration) from an area (range resolution cell) characterized by the scattering matrix $[\mathbf{S}]$ can be expressed, for each pixel, as a function of $[\mathbf{S}]$, the distortions matrices, the slant range r , and the target illumination angle θ by (Touzi et al., 1993; Freeman, 1991)

$$[\mathbf{V}] = \mathcal{L}' \frac{1}{r} \{ [\mathbf{d}^r]^T [\mathbf{g}(\theta)]^T \cdot [\mathbf{S}] \cdot [\mathbf{g}(\theta)] [\mathbf{d}^t] \} \quad (38)$$

where \mathcal{L}' is a constant that depends on the system parameters; $[\mathbf{d}^r]$ and $[\mathbf{d}^t]$ are the distortion matrices at the receiving and transmitting system, respectively, constructed from the switch distortion matrix and the complex gains of the H–V signal paths; and $[\mathbf{g}(\theta)]$ is the antenna distortion matrix at the illumination angle θ (Touzi et al., 1993). The voltage of Equation (38) was derived for a satellite SAR, thus explaining the reason that \mathbf{V} is inversely proportional to r (and not to r^2) (for more details, see Touzi et al., 1993; and Freeman, 1991).

To synthesize σ^0 for any combination of transmitting–receiving antenna polarizations, pure H and V polarizations should be extracted from the distorted voltage measurements. Many techniques of calibration have been developed for the various existing systems. Most of these techniques require the use of reference point targets. Van Zyl (1990) was the first to introduce the use of extended natural targets for polarimeter calibration and showed that the particular properties of azimuthally symmetric targets established by Borgeaud et al. (1987) can be used to simplify the calibration algorithm and reduce the number of reference point targets required for calibration. This idea (Van Zyl, 1990) has served as the basis for the development of most calibration methods since (Luscombe et al., 2000; Freeman, 1995; Quegan, 1993; Shimada, 2001; Touzi et al., 1993).

Calibration of systems with antennas of relatively low H–V polarization isolation is generally much more complex than that for systems with highly isolated antennas. Antennas of low H–V isolation, such as the AirSAR antenna (Van Zyl, 1990) and Pi-SAR (Wakabayashi et al., 2001) (about 23 dB isolation), manifest a significant crosstalk term that varies with incidence angle. Measurement of the variation of the antenna crosstalk term with incidence angle would require the deployment of many reference point targets along the whole swath, which is not convenient in practice. The method of Van Zyl (1990) based on the use of various azimuthally symmetric natural targets selected within the antenna look-angle range provides an excellent solution to such a complex problem. This method, which has been widely validated, is the standard method for removal of antenna crosstalk. At the presence of significant topographic relief, a digital elevation model is needed for calibration of polarimeters with antennas of low isolation (Van

Zyl et al., 1992; 1993). Calibration of systems with highly isolated antennas (better than 30 dB; Touzi et al., 1993) is much easier because the unknown calibration parameters do not vary with incidence angle. Internal signal measurement (channel complex gain offset) during data acquisition is strongly recommended to avoid the deployment of reference point targets at each data acquisition (Christensen et al., 1998; Touzi, 1999a; Touzi and Livingstone, 2003).

Calibration of the first satellite polarimetric SAR mission, SIR-C, needed the development of a specific methodology (Freeman, 1995; Sarabandi et al., 1995). New problems had to be solved related to the active nature of the SIR-C antenna, such as nonreciprocity introduced by the transmit/receive active elements and short- and long-term variations of antenna parameters. The lessons learned from SIR-C (Freeman, 2003) should help the calibration of future satellite polarimetric SARs, such as RADARSAT-2 (Luscombe et al., 2000), ALOS-PALSAR (Ito et al., 2001), and TerraSAR X and L-bands (Schwerdt et al., 2003; Mathew, 2001).

All these calibration methods require the complex radar signal parameters received from reference point targets to be measured. The intensity integration method, which is robust to system focus-setting errors (Gray et al., 1990), was used to estimate point target energy, and the phase of the peak signal was taken as an estimate of the signal phase (Freeman, 1992). In 1992, Touzi (1992) and Touzi et al. (1992b) showed that the latter method, referred to as the peak method, was sensitive to system focus-setting errors. They introduced the complex integration method (CIM) for a robust estimation of both intensity and phase of point target signal. The CIM is now used at CCRS within the calibration package developed for the X- and C-band Convair-580 SAR systems (Touzi et al., 1993; Livingstone et al., 1995; Hawkins, 1990; Touzi and Livingstone, 2003). The calibration method (Touzi et al., 1993), which was inspired by the Van Zyl method (Van Zyl, 1989) and uses the CIM for measurement of point target signal parameters, leads to a calibration accuracy of within 1–2 dB in radiometry and 5° in phase (Hawkins et al., 1999; Touzi and Livingstone, 2003).

Most of the existing systems achieve an accuracy in radiometry of within 1–2 dB and in phase within 10° (Freeman, 1992; Touzi et al., 1993; Christensen et al., 1998; Touzi and Livingstone, 2003), which satisfies the list of calibration requirements set for SIR-C (Dubois, 1992). With the continuous advance of technology, future systems should provide better accuracy, and the list of calibration requirements (Dubois and Norikane, 1987) that has been used for SIR-C, RADARSAT 2, and ALOS should be updated (Touzi et al., 2003). The list should also specify the Faraday rotation error tolerated for L- and P-band systems. Calibration of the Faraday rotation at L- and P-bands is the hot topic. Faraday rotation is a significant source of errors that may affect observations made by L-band SARs, such as ALOS-PALSAR and TerraSAR (Rignot, 2000; Freeman and Saatchi, 2004; Freeman, 2004; Wright et al., 2004). With the closing launch of ALOS, intense attention has been given to modeling the Faraday rotation

angles and its effects on received intensity (Wright et al., 2003; Freeman and Saatchi, 2004) and calibration of polarimetric SAR subject to Faraday rotation (Freeman, 2004). Freeman has fixed a calibration requirement of 2.5° on the maximum residual Faraday rotation angle error (Touzi et al., 2003), according to the excellent papers (Freeman and Saatchi, 2004; Freeman, 2004) being published on the calibration of systems operating at wavelengths subject to Faraday rotation errors.

Polarization information extraction using the scattered and received wave parameters

One-look and multilook SAR data processing

The principle of synthesizing in azimuth a larger aperture than the actual antenna size requires the integration of target measurements under coherent conditions (Curlander and McDonough, 1991; Raney, 1998). If the azimuth integration time is much smaller than the target coherence, integration over the Doppler bandwidth yields a resolution close to the half width of the antenna (Curlander and McDonough, 1991; Raney, 1998). This resolution is degraded under partial coherence conditions (Raney, 1980), and the partially coherent received wave can no longer be fully characterized with the scattering matrix, as seen in the earlier sections titled “Quasi-monochromatic and partially polarized waves” and “Coherency matrix for the representation of partially polarized waves”. To retrieve the full polarization information of partially coherent signals, integration might be completed under coherence conditions, within separate small Doppler bandwidths (single looks of shorter integration time), similar to that for one-channel conventional SARs (Raney, 1980; Engen and Johnson, 1995). Comparison of the single-looks scattering matrix measurement leads to a better characterization of the illuminated partially coherent targets, as in Engen and Johnson (1995), Ainsworth et al. (1999), Ferro-Famil et al. (2003), and Souyris et al. (2004).

In practice, polarimetric SAR processing is completed for each channel HH, HV, VH, and VV, under the assumption that the received signal is coherent (i.e., completely polarized wave), and a high-resolution one-look image is generated under the Sinclair matrix [S] forma (Dubois and Norikane, 1987; Van Zyl et al., 1987a). Multilook (L) processing can also be achieved to reduce the volume of the image data. In this case, the L scattering matrices of the various single looks are processed, and the averaging is conducted under the Kennaugh matrix format to preserve the fully polarimetric information (Dubois and Norikane, 1987; Van Zyl et al., 1987a; Zebker and Van Zyl, 1991).

Scattered wave parameters

Scattered intensity extrema of a completely polarized wave

The information provided by the scattered wave power extrema might be useful for characterization of the illuminated

target. If the scattered wave is completely polarized, the polarimetric information is fully characterized with the scattering matrix [S]. The total power P_s backscattered from the target is expressed by Equation (20) as a function of the Graves matrix [G]. The extrema of P_s correspond to the real eigenvalues of the Hermitian positive semi-definite matrix [G], which are obtained at the orthogonal eigenvectors polarizations of [G] (Graves, 1956; Kostinski and Boerner, 1986). The maximum backscattered power, which is equal to the largest eigenvalue of [G], is reached when the polarization of the transmitting antenna is identical to the eigenvector of [G] for the largest eigenvalue. The maximum backscattered power is equal to the maximum received power when the transmitting and receiving antennas are of the same polarization (Kennaugh, 1951). In fact, this maximum is identical to that obtained in the general case (transmitting and receiving antennas might be of different polarizations), as stated in Kennaugh (1951) and justified later theoretically by Kostinski and Boerner (1986) using their three-stage optimization method.

Contrast optimization of a completely polarized wave

The Graves method (Graves, 1956) was extended to contrast optimization (Kostinski and Boerner, 1987). If P_A and P_B are the energies backscattered from two targets A and B, the contrast Cont to be optimized might be expressed as a function of the Graves matrices [G_A] and [G_B] using Equation (21) as (Kostinski and Boerner, 1987)

$$\text{Cont} = \frac{(\vec{p}^t)^{*T} \cdot [\mathbf{G}_A] \cdot \vec{p}^t}{(\vec{p}^t)^{*T} \cdot [\mathbf{G}_B] \cdot \vec{p}^t} \quad (39)$$

The extrema are given by the so-called Rayleigh-Ritz coefficients, which are the eigenvalues of the generalized eigenvector equation

$$[\mathbf{G}_A] \vec{x} = \lambda [\mathbf{G}_B] \vec{x} \quad (40)$$

Unfortunately, both techniques based on the Graves matrix can only be applied to completely polarized scattered waves that are fully characterized by [S] and as such are of limited application. Solutions for partially polarized waves are presented in a later section titled “Extrema of the degree of polarization and extrema of the total scattered intensity”.

Completely polarized and completely unpolarized components of a partially polarized scattered wave

The Stokes vector of the scattered wave might be expressed as the sum of the Stokes vectors of the completely polarized and completely unpolarized components (Born and Wolf, 1959), thus leading to the following expression as a function of the degree of polarization p of Equation (14) and the coordinates (R_0, R_1, R_2, R_3) of the scattered wave Stokes vector (Ko, 1962; Poelman and Guy, 1984; Van Zyl et al., 1987a; Kostinski and Boerner, 1988; Evans et al., 1988):

$$\bar{S}_{sc}^T = (pR_0, R_1, R_2, R_3)^T + [(1-p)R_0, 0, 0, 0]^T \quad (41)$$

Ko (1962), Poelman and Guy (1984), and Kostinski and Boerner (1988) associated a high importance to the first term pR_0 , which corresponds to the completely polarized backscattered signal. In contrast to the unpolarized noiselike component, this term represents adjustable intensity that can be fully matched by an adapted receiving antenna (Ko, 1962; Poelman and Guy, 1984; Kostinski and Boerner, 1988). This leads to a received scattering with a maximum completely polarized component (and minimum completely unpolarized component) whose parameters can be characterized more efficiently than those of the original received signal. This optimization process was the basis for the optimum clutter-suppression method introduced by Poelman and Guy (1984). The completely polarized component of the clutter to be suppressed is maximized, and the receiving antenna polarization is set orthogonal to the maximum completely polarized component. In this way, the average received power is identical to half of the average power contained in the completely unpolarized component of the returned wave, which has been minimized (Poelman and Guy, 1984; Kostinski and Boerner, 1988). Since the generation of pR_0 extrema for each pixel of the scene under study is quite expansive in computing time, Kostinski and Boerner (1988) derived an analytical method for the extraction of the extrema of the completely polarized component from the sample Mueller matrix. They showed that the problem is equivalent to solving numerically a six-order polynomial equation, and thus significantly reducing the computing time when compared with the systematic method, which consists of deriving the extrema with the polarization ellipse angles ψ and χ sampled at 1° .

Evans et al. (1988) synthesized the extrema of the completely polarized and completely unpolarized components for various extended targets including urban areas, parks, and ocean in the San Francisco image. These parameters provided interesting information on the type and homogeneity of the scattering and demonstrated the great potential of polarimetric information in target discrimination (Evans et al., 1988). Unfortunately, this work has never been continued, and there is still a lot to learn about the information provided by these components, especially by the unpolarized component whose information is still unknown.

Extrema of the degree of polarization and extrema of the total scattered intensity

The degree of polarization was qualified in Jones (1947) and Wolf (1959) as the most important parameter associated with the state of partial polarization of scattered waves. The clutter-suppression algorithm of Poelman and Guy (1984) used the degree of polarization to assess the limit of clutter-suppression capability. Touzi et al. (1992a) have also associated great importance to this parameter, and an analytical method was developed for the calculation of the extrema of the degree of polarization, given a Mueller or Kennaugh matrix sample. It was shown that the problem is equivalent to numerically

solving a six-order polynomial equation (Touzi et al., 1992a). Compared with the systematic method, the analytical method permits saving about 50% of computing time. In addition, the analytical method is more accurate than the systematic method, which might lead to erroneous results because of the sampling interval (generally 1° in χ and ψ). The analytical method also permits generating the optimum transmitted polarization, which maximizes the degree of polarization of the scattered wave, and as a result maximizes the intensity of the completely polarized component of the backscattered and received intensity (Touzi et al., 1992a). This method is used in Touzi et al. (2004a) to generate the wave polarization anisotropy that was introduced in Touzi (2000) and was shown to be effective for ship detection (Touzi, 2000; Touzi et al., 2004a).

The expressions of the extrema of the total scattered intensity R_0 were also derived by Touzi et al. (1992a). A combination of the extrema of the degree of polarization and the extrema of the scattered intensity permits a successful and efficient unsupervised classification of the San Francisco image as a function of the target scattering type and homogeneity (Touzi et al., 1992a; 2004b).

Received wave parameters

Polarization signature

To extract full polarization information, the target coefficient of variation σ^0 can be synthesized for all combinations of transmitting–receiving antenna polarizations. The polarization signature was introduced in Van Zyl et al. (1987a) and Agrawal and Boerner (1989) as a convenient graphical representation of the variation of the received scattering cross section as a function of the transmitting antenna polarization. The polarization response is a plot of received intensity as a function of the ellipse polarization angles (ψ , χ). When the same polarization is used for transmitting and receiving polarization, the plot is referred to as the copolarized signature. When they are orthogonal, the cross-polarized signature is obtained. It is now well accepted that the polarization signature is quite useful for describing polarization properties of points and distributed targets (Van Zyl et al., 1987a; Evans et al., 1988; Ulaby and Elachi, 1990). The polarization signature might also be useful for the measurement of ship orientation angle (Touzi, 1999b) and the extraction of the orientation angle induced by azimuthal slopes (Schuler et al., 1996) for topography measurement (Schuler et al., 2000).

The pedestal of the polarimetric signature may also be a worthy source of information for target characterization (McNairn et al., 2002). In fact, the pedestal corresponds to the ratio of the received power extrema when the antennas are copolarized or cross-polarized. Therefore, the pedestal provides information equivalent to that obtained with the coefficient of variation by Van Zyl et al. (1987a). The latter should be more effective because it is not limited to copolarizations and cross-polarizations.

Circular polarizations

Circular right–right (RR) and right–left (RL) polarizations were widely used for the remote sensing of precipitation (McCormick and Hendry, 1973; McCormick, 1996; Antar et al., 1992). The ability of these polarizations to enhance the even bounces (with RR polarization) and odd bounces (with RL polarizations) makes them very effective in rain measurements. The radar backscattered at circular polarizations was also successfully used for ship detection (Touzi, 1999b; Touzi et al., 2004a) and forest type discrimination (Touzi et al., 2004b). Another source of information is the coherence of the RR and LL circular polarization, which has been found to be extremely sensitive to surface roughness (Mattia et al., 1997). Schuler et al. (2002) have investigated the RR–LL coherence for azimuth slope measurement.

As in the case of the phase difference of the horizontal and vertical polarizations $\phi_{HH} - \phi_{VV}$, which was shown to provide useful information for target characterization (Foo et al., 1990; Sarabandi, 1992; Ulabi and Elachi, 1990), the information provided by the phase difference between RR and LL circular polarizations is worth investigating. The RR–LL phase difference has been exploited in Lee et al. (2000; 2002a) to measure the orientation angle θ induced by azimuthal slopes. Lee et al. showed that θ (for $0 \leq \theta \leq \pi/4$) might be extracted from the RR–LL phase difference of the radar signal return from a terrain surface as

$$\begin{aligned} -4\theta &= \arg(\langle S_{RR} S_{LL}^* \rangle) \\ &= \arctan \left[\frac{-4 \langle \text{Re}(S_{HH} - S_{VV}) S_{HV}^* \rangle}{-\langle |S_{HH} - S_{VV}|^2 \rangle + 4 \langle |S_{HV}|^2 \rangle} \right] \end{aligned} \quad (42)$$

When a polarimetric radar images a terrain surface with significant relief, the change in the polarization orientation angle is geometrically related to the topographical slopes and the radar illumination angle by

$$\tan \theta = \frac{\tan \omega}{-\tan \gamma \cos \phi + \sin \phi} \quad (43)$$

where ϕ is the radar illumination angle, $\tan \omega$ is the azimuth slope, and $\tan \gamma$ is the slope in the ground range direction (Lee et al., 2000). Polarimetric imaging radar derived orientation angles have been successfully applied at L- and P-bands to measure topography (Schuler et al., 2000; 2002; Lee et al., 2002a) and are used for polarimetric SAR data compensation to ensure accurate estimation of geophysical parameters in rugged terrain areas (Lee et al., 2000). The method of Lee and Schuler was successfully validated for L- and P-band polarimetric SAR data but is less effective at C-band or higher frequency SAR data (Schuler et al., 2002; Lee et al., 2002a).

Received wave intensity parameters

The received power can be expressed as a function of the total intensity R_0 and the degree of polarization p of the backscattered wave as

$$P_{\text{rec}} = pR_0 \cos^2\left(\frac{\delta}{2}\right) + \frac{R_0}{2}(1-p) \quad (44)$$

where δ is the angular distance on the Poincaré sphere between the polarization state of the scattered wave and the received wave (Ko, 1962). The received power is maximum when the received antenna polarization is matched to the scattered wave ($\delta = 0$ and $P_{\text{rmax}} = (1+p)R_0/2$). The received power is minimum when the received antenna polarization is orthogonal to the polarization of the scattered wave ($\delta = \pi$ and $P_{\text{rmin}} = (1-p)R_0/2$). Antenna-backscattered wave matching (or cross-matching) served as the basis for the development of the multinock logic-product suppression filter (Poelman and Guy, 1984) and the three-stage optimization technique derived in Kostinski and Boerner (1986).

Evans et al. (1988) used the extrema of the received wave intensity to separate cover types. Van Zyl et al. (1987a) used the ratio of the extrema of the received power, referred as to the coefficient of variation, as an indicator of spatial target heterogeneity and to assess the complexity of target scattering mechanisms (Evans et al., 1988). Various combinations of the extrema of the received of power, named the fractional polarization, were used and validated with the same potential by Zebker et al. (1987).

The received intensity extrema can be derived by systematically varying the polarization angles (ψ_t, χ_t) of the transmitted wave polarization. A less expansive computing time solution might be used in the particular case of transmitting and receiving antennas of the same polarization. Based on the Mueller matrix approach, Van Zyl et al. (1987b) have shown that this problem is equivalent to solving a six-order polynomial equation that can be solved numerically. Tragl (1990) used the covariance matrix approach to show that the received mean power in the copolarized radar channel is bounded by the largest and the smallest eigenvalues of the Hermitian positive semi-definite covariance matrix $[C]$ of Equation (36).

Received intensity contrast optimization

For a completely polarized wave, the solution obtained in the section titled “Contrast optimization of a completely polarized wave” can be used under the assumption that the transmitting and receiving antennas are of the same polarization. More general algorithms were derived in the case of partially polarized waves (Ionnidis and Hammers, 1979; Swartz et al., 1988). The received powers in the contrast ratio were expressed (Swartz et al., 1988) as a function of the target covariance matrices $[C_A]$ and $[C_B]$, using Equation (36). The contrast extrema are obtained by solving the generalized eigenvector equation (Swartz et al., 1988)

$$[C_A]\vec{x} = \lambda[C_B]\vec{x} \quad (45)$$

An analytical solution was derived in Swartz et al. (1988) for the simplified problem of contrast optimization of azimuthally symmetric targets.

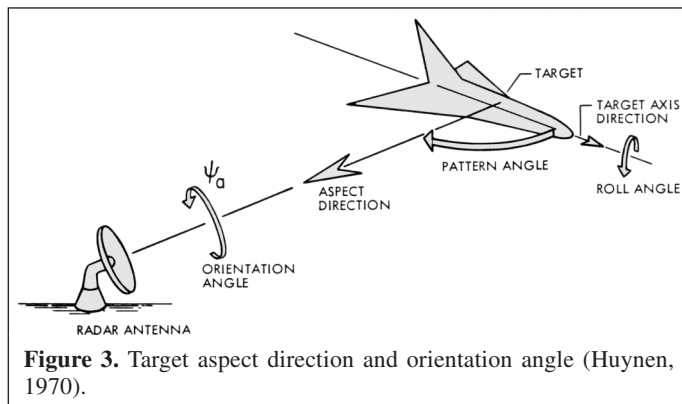
Coherent and incoherent target decomposition

The objective of target decomposition theory is to express the average scattering mechanism as the sum of independent elements to associate a physical mechanism with each component (Huynen, 1965; Cloude and Pottier, 1996). Two theories of target decomposition can be distinguished: coherent target decomposition (CTD) and incoherent target decomposition (ICTD). CTD was developed to characterize completely polarized scattered waves for which the fully polarimetric information is contained in the scattering matrix. Many CTD methods were published (Huynen, 1965; Krogager, 1990; Cameron et al., 1996; Touzi and Charbonneau, 2002; Corr and Rodrigues, 2002). In the following section, the Kennaugh–Huynen CTD (Kennaugh, 1951; Huynen, 1965), the Cameron CTD (Cameron et al., 1996), and the symmetric scattering characterization method (SSCM) (Touzi and Charbonneau, 2002) developed for optimization of target coherent symmetric scattering are presented. ICTD is summarized in a later section of the paper.

Coherent target decomposition

Kennaugh–Huynen coherent decomposition

Target radar return depends on the illumination angle, named aspect angle in Huynen (1970), and the so-called target orientation angle as presented in **Figure 3** (Huynen, 1970). The orientation angle ψ_a is referred to as the target axis orientation angle because it determines the target orientation with reference to the line of sight (LOS) direction. Subtracting the effect of the geometrical motion parameter ψ_a on the target scattering should lead to a presentation of the scattering matrix under an orientation invariant form that fully characterizes



target parameters (Kennaugh, 1951; Huynen, 1965). The properties of the scattering matrix that are independent of special matrix representations are generally studied by solving the eigenvalue problem (the characteristic decomposition) (Wiener, 1930). Solutions to the eigenvalue problem are expressed by eigenvalues and eigenvectors, and it is expected that the properties of these may be associated with the physical properties of radar targets.

The scattering matrix $[S]$ can be diagonalized if $[S]$ is symmetric and nonsingular. $[S]$ has two complex eigenvalues, λ_1 and λ_2 , which correspond to two eigenvectors that are not generally orthogonal. To represent the information in an orthonormal basis, the characteristic decomposition might be completed in the power form using the Graves power matrix $[G]$ of Equation (21). Diagonalization of the Hermitian positive semi-definite matrix $[G]$ leads to a decomposition in an orthonormal eigenvector basis, with positive real eigenvalues μ_1 and μ_2 that are the magnitude square of the $[S]$ eigenvalues: $\mu_i = |\lambda_i|^2$. Unfortunately, the $[G]$ diagonalization process leads to an incoherent target scattering decomposition, since the diagonalized power matrix obtained has real (non-complex) eigenvalues μ_1 and μ_2 .

To fully exploit the information provided by coherent scattering, the characteristic decomposition should be applied on the $[S]$ matrix using a non-conventional diagonalization procedure that leads to a diagonalization of the matrix in an orthonormal vector basis. The theorem of Takagi (1927) was used for this purpose in Kennaugh (1951) and Huynen (1970), and the so-called con-diagonalization was applied to the $[S]$ matrix for a coherent target decomposition in an orthonormal vector basis. Under the condition that $[S]$ is a symmetric matrix, S can be unitarily con-diagonalized;⁵ $[S]$ can be transformed into a diagonal form by a unitary transformation in the con-eigenvectors also known as Kennaugh's pseudo-eigenvalues equation (Takagi, 1927; Kennaugh, 1951; Huynen, 1970; Hong and Horn, 1988; Lüneburg, 2002):

$$[S]\vec{x} = \lambda\vec{x}^* \quad (46)$$

The con-eigenvectors are “true” eigenvectors of the eigenvector equation expressed in terms of the Graves matrix $[G]$:

$$[G]\vec{x} = \mu\vec{x} \quad (47)$$

$[G]$ eigenvalues that might be derived from Equation (47) are identical to the magnitude square of $[S]$ con-eigenvalues; $\mu_i = |\lambda_i|^2$ for $i = 1, 2$ (Kennaugh, 1951; Huynen, 1970; Kostinski and Boerner, 1986). It is worth noting that the con-diagonalization might lead to a degenerated case, which should be considered with care, when the con-eigenvalues λ_1 and λ_2 coincide (Hong and Horn, 1988; Lüneburg, 1995a; 2002).

Kennaugh (1951) and later Huynen (1965; 1970) used Takagi's con-diagonalization as the basis of the so-called Kennaugh–Huynen CTD. This CTD permits the representation

⁵The prefix con means conjugation (Hong and Horn, 1988; Lüneburg, 2002).

of the scattering matrix $[\mathbf{S}]$ in term of parameters that are independent of the target orientation angle. Under the reciprocity assumption, the scattering matrix can be con-diagonalized in the orthonormal con-eigenvectors basis as (Kennaugh, 1951; Huynen, 1970)

$$[\mathbf{S}] = [\mathbf{R}(\psi_a)][\mathbf{Tr}(\tau_m)] \cdot [\mathbf{S}_d] \cdot [\mathbf{Tr}(\tau_m)][\mathbf{R}(-\psi_a)] \quad (48)$$

where $[\mathbf{R}(\psi_a)]$ is the rotation transformation matrix of angle ψ_a , $[\mathbf{S}_d]$ is a diagonal matrix with the $[\mathbf{S}]$ con-eigenvalues λ_1 and λ_2 as diagonal elements, and $[\mathbf{Tr}]$ is given by

$$[\mathbf{Tr}] = \begin{bmatrix} \cos \tau_m & -j \sin \tau_m \\ -j \sin \tau_m & \cos \tau_m \end{bmatrix} \quad (49)$$

The con-eigenvectors are orthogonal and given by (Kennaugh, 1951; Huynen, 1970)

$$\begin{aligned} \vec{m}(\psi_a, \tau_m) &= [\mathbf{R}(\psi_a)] \cdot (\cos \tau_m, j \sin \tau_m) \\ \vec{m}^\perp(\psi_a, \tau_m) &= \vec{m}(\psi_a + \pi/2, -\tau_m) \\ &= [\mathbf{R}(\psi_a)] \cdot (-j \sin \tau_m, \cos \tau_m) \end{aligned} \quad (50)$$

The pseudo-eigenvector \vec{m} , which corresponds to the maximum return $|\lambda_1|^2$ (i.e., $|\lambda_1| > |\lambda_2|$), is named the “maximum polarization” (Kennaugh, 1951; Huynen, 1970). ψ_a and τ_m are the orientation and ellipticity angles, respectively, of the maximum polarization. ψ_a is as such the rotation angle (a pure geometrical parameter) to be applied to subtract the effect of the orientation angle on the target scattering. ψ_a is equivalent to the orientation angle of Equation (42) used by Lee et al. (2002a) and Schuler et al. (2002) for azimuth slope measurement. The helicity angle τ_m (Huynen, 1970) is used to assess target symmetry (Kennaugh, 1951; Huynen, 1970).

The con-diagonalization leads to complex con-eigenvalues noted as $\lambda_1 = m \exp 2j(\nu + \rho)$ and $\lambda_2 = m \tan 2(\gamma) \exp -2j(\nu - \rho)$. The characteristic angle γ ($0 \leq \gamma \leq 45^\circ$ so that $|\lambda_1|$ has the largest value) is also known as the polarizability angle (Huynen, 1970). The relative phase ν ($-45^\circ \leq \nu \leq 45^\circ$) is referred to as the target skip angle, since its values have some relationship to depolarization because of the number of bounces of the reflected signal (Huynen, 1970). The absolute phase of the target is ρ . All of these independent parameters, known as the Huynen parameters, permit a full target characterization and were used as the basis of the polarization invariant Huynen fork introduced in Huynen (1970).

SSCM for characterization of symmetric target scattering

Symmetric scattering decomposition

Kennaugh (1951) and Huynen (1965) associated importance with a class of targets termed symmetric. A symmetric target is a target having an axis of symmetry in the plane orthogonal to the radar LOS (Kennaugh, 1951; Huynen, 1965). Symmetric targets have a scattering matrix that can be diagonalized by a rigid rotation about the LOS, as seen from Equation (50) with

$\tau_m = 0$ (Kennaugh, 1951; Huynen, 1965). Lüneburg (1995b) has shown that the symmetric scatter matrix $[\mathbf{S}]$ can be diagonalized by a rigid rotation if $[\mathbf{S}]$ is normal; $[\mathbf{S}][\mathbf{S}]^{*T} = [\mathbf{S}]^{*T}[\mathbf{S}]$. Cameron et al. (1996) developed an algorithm that maximizes the symmetrical component of coherent scattering, which is then expressed as the sum of independent elements so as to associate a physical mechanism with each component. For operational use of their CTD, Cameron et al. (1996) introduced a classification method that has been widely used for characterization and identification of point targets such as ships (Jeremy et al., 2001) and small planes (Rais and Mansfield, 1999). Unfortunately, it was shown in Touzi and Charbonneau (2002) that the coarse classification of Cameron et al. (1996) might be misleading because of the significant radiometric dispersion that is tolerated (up to ± 8 dB) and the absence of criteria that avoid the application of the CTD method in areas of noncoherent scattering. A new method, named the symmetric scattering characterization method (SSCM), was introduced in Touzi and Charbonneau (2002) for a high-resolution characterization of target symmetric scattering under coherent conditions. The SSCM is summarized in the following.

Maximization of symmetric scattering: Cameron's CTD

Under target and SAR system reciprocity assumptions, the target scattering matrix is expressed in terms of the Pauli matrices σ_i as (Cameron et al., 1996)

$$[\mathbf{S}] = \alpha \cdot [\sigma_0] + \beta \cdot [\sigma_1] + \gamma \cdot [\sigma_2] \quad (51)$$

where the Pauli spin matrices are

$$\sigma_0 = \frac{1}{\sqrt{2}} \begin{bmatrix} 1 & 0 \\ 0 & 1 \end{bmatrix} \quad (52)$$

$$\sigma_1 = \frac{1}{\sqrt{2}} \begin{bmatrix} 1 & 0 \\ 0 & -1 \end{bmatrix} \quad (53)$$

$$\sigma_2 = \frac{1}{\sqrt{2}} \begin{bmatrix} 0 & 1 \\ 1 & 0 \end{bmatrix} \quad (54)$$

Scattering is symmetric if there exists an angle of rotation ψ_a , referred to as the target orientation angle (Huynen, 1970; Cameron et al., 1996), which cancels the projection of $[\mathbf{S}]$ of Equation (51) on the nonsymmetric Pauli direction $\vec{\sigma}_2$ (where $\vec{\sigma}_2$ is the vectorial form of the Pauli matrix $[\sigma_2]$). This leads to the following expression for the symmetric part, \vec{S}_{sym} , as a function of the angle $\theta = -2\psi_a$ (Cameron et al., 1996; Touzi and Charbonneau, 2002):

$$\vec{S}_{\text{sym}} = \alpha \vec{\sigma}_0 + \epsilon \cdot [\cos \theta \cdot \vec{\sigma}_1 + \sin \theta \cdot \vec{\sigma}_2] \quad (55)$$

The symmetric component \vec{S}_{sym} of the total scattering \vec{S} (the vector form of $[\mathbf{S}]$) reaches its maximum for the angle θ , which

satisfies the following relationship for $\beta \neq \gamma$ (Cameron et al., 1996; Touzi and Charbonneau, 2002):

$$\tan(2\theta) = \frac{\beta\gamma^* + \beta^*\gamma}{|\beta|^2 - |\gamma|^2} \quad (56)$$

After diagonalization, the largest symmetric component $\vec{S}_{\text{sym}}^{\text{max}}$ can be expressed in the trihedral–dihedral basis, $(\vec{\sigma}_0, \vec{\sigma}_1)$, as

$$\vec{S}_{\text{sym}}^{\text{max}} = \alpha\vec{\sigma}_0 + \epsilon\vec{\sigma}_1 \quad (57)$$

where ϵ is given: $\epsilon = (\beta \cos \theta + \gamma \sin \theta)$.

Target Poincaré sphere

The target Poincaré sphere was introduced in Touzi and Charbonneau (2002) for the high-resolution mapping of symmetric scattering. Per analogy with the wave Poincaré sphere of the earlier section titled “Stokes vector”, the normalized diagonalized symmetric scattering $\vec{\Lambda} = \vec{S}_{\text{sym}}^{\text{max}} / \|\vec{S}_{\text{sym}}^{\text{max}}\|$ is expressed as a function of the target Poincaré sphere angles ψ_c and χ_c as

$$\vec{\Lambda} = [1 \cos(2\chi_c) \cos(2\psi_c) \cos(2\chi_c) \sin(2\psi_c) \sin(2\chi_c)] \quad (58)$$

where ψ_c and χ_c are derived as a function of the target parameters α and ϵ of Equation (57). To remove the rotation phase ambiguity (Huynen, 1970; Cameron et al., 1996), only half of the sphere is used, with ψ_c varying within the interval $[0, \pi/2]$ (Touzi and Charbonneau, 2002). Each coherent symmetric scatterer is uniquely mapped as a point of latitude $2\psi_c$ and longitude $2\chi_c$ on the surface of the target Poincaré sphere presented in **Figure 4**. The normalized scattering vectors of the quarter-wave devices are on the north and south poles. The

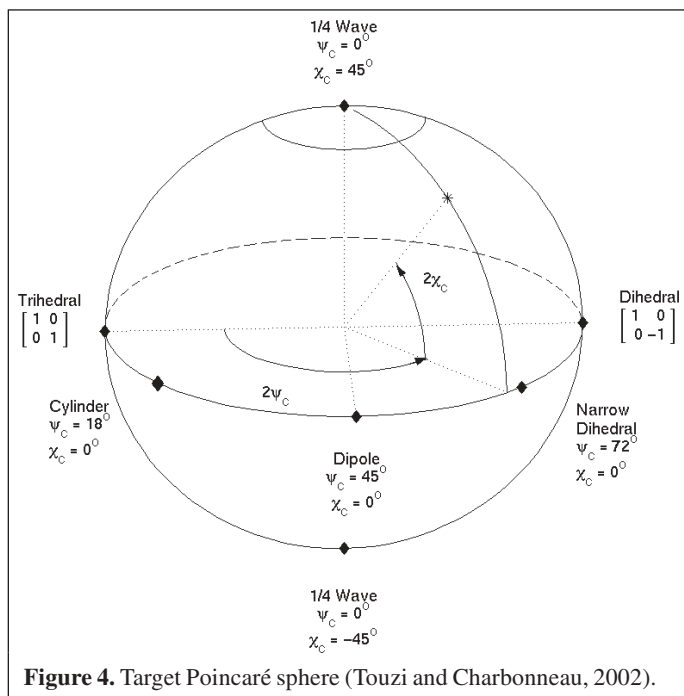


Figure 4. Target Poincaré sphere (Touzi and Charbonneau, 2002).

normalized scattering vectors of the trihedral $\vec{\sigma}_0$, diplane $\vec{\sigma}_1$, dipole \vec{S}_1 , cylinder \vec{S}_{cy} , and narrow diplane \vec{S}_{nd} are on the equator.

A partially coherent symmetric scatterer is represented as a point inside the sphere at a distance from the sphere centre determined by the degree of coherence, p_{sym} , which was defined by Touzi and Charbonneau (2002) as

$$p_{\text{sym}} = \frac{\sqrt{(\langle |\alpha|^2 - |\epsilon|^2 \rangle)^2 + 4|\langle \alpha \cdot \epsilon^* \rangle|^2}}{\langle |\alpha|^2 + |\epsilon|^2 \rangle} \quad (59)$$

The degree of coherence p_{sym} was shown to be an efficient tool for the assessment of distributed target scattering coherence (Touzi and Charbonneau, 2002); p_{sym} permits the separation of coherent scattering targets from targets of partially coherent scattering, prior to the application of the SSCM, which should be limited to the characterization of coherent scattering (Touzi and Charbonneau, 2002).

SSCM scheme for optimum characterization of symmetric scattering

The SSCM includes the following steps (Touzi and Charbonneau, 2002): (i) calculation of the parameters α and ϵ of the maximum symmetric component, using the CTD of Cameron et al. (1996); (ii) classification of distributed target scattering into coherent and noncoherent classes using p_{sym} information; (iii) classification of point target scattering into coherent and noncoherent classes using the Rician threshold (Touzi and Charbonneau, 2002); and (iv) computation and analysis of the target Poincaré sphere parameters within the coherent class.

The SSCM was applied successfully in Touzi and Charbonneau (2003) and Touzi et al. (2004a; 2004c) for ship identification and ship motion angle measurement. The use of the scatterer coordinates on the target Poincaré sphere enabled the selection of potential symmetric targets on the ship that can be assigned as the ship’s signature and permit a pitch angle measurement within 0.2° accuracy (with reference to the ground measurements).

Incoherent target decomposition

The aforementioned CTD methods can only be applied to coherent scattering. Generally, the scattered wave is partially polarized and the user might be interested in the extraction of geophysical parameters from an area that exhibits significant natural variability in the scattering properties (Van Zyl, 1992). A unique decomposition of the target-averaged Stokes or covariance matrix into a sum of matrices representing single scatterers should lead to a more accurate interpretation of the scattering processes and make easier the extraction of geophysical parameters from the measured radar data (Cloude and Pottier, 1996; Van Zyl, 1992).

One of the first examples of such a target decomposition technique was provided by Chandrasekhar (1960). Considering the case of lateral scattering of light of small anisotropic

particles, Chandrasekhar decomposed the total average phase matrix into the sum of a Mueller matrix that represents the sum of a dipole scattering Mueller matrix and a Mueller matrix that represents pure random scattering. As such, his target decomposition followed the same principle that breaks the Stokes vector of a partially polarized wave into the sum of a Stokes vector representing a fully polarized wave and a Stokes vector representing a completely unpolarized wave (Chandrasekhar, 1960; Van Zyl, 1992). Huynen (1970) also introduced a target decomposition theorem in which he decomposed an average Mueller matrix into the sum of a Mueller matrix for a single scatterer and a noise or N -target Mueller matrix. Unlike Chandrasekhar's decomposition, however, Huynen's N -target is not polarization independent and has been shown to be just one of an infinite set of such residue matrices, meaning that Huynen decomposition is not unique (Cloude, 1992; Van Zyl, 1992; Cloude and Pottier, 1996).

The use of the characteristic decomposition of target covariance (Equation (29)) and coherency (Equation (30)) matrix for incoherent target decomposition was introduced by Cloude (1986). This was an extension of Wiener's (1930) characteristic decomposition of the wave coherency matrix to the target coherency matrix. Wiener used the characteristic decomposition of wave covariance matrix for an in-depth analysis of the eigenvalue spectrum of optic waves. Cloude's decomposition was shown to be unique and, in the monostatic case, breaks the average covariance matrix up to the weighted sum of three covariance matrices representing three different single scatterers. Cloude applied his decomposition on the target coherency matrix in the basis formed by the Pauli spin matrices and concluded that decomposition can be done using any four complex matrices that satisfy the constraint of completeness and normalization (Cloude, 1986; Cloude and Pottier, 1996; 1997a). Van Zyl (1992) extended Cloude's work and applied the decomposition to the target covariance matrix as the sum of statistical uncorrelated single scattering represented by the orthonormal covariance eigenvectors. Van Zyl validated the great potential of the incoherent target decomposition for analysis and interpretation of forest scattering using AirSAR data.

The characteristic decomposition of the target covariance and coherency matrices leads to the same eigenvalues that are positive and real (Cloude and Pottier, 1996). Both characteristic decompositions yield orthonormal eigenvectors, which are used to analyze the eigenvector spectrum (Wiener, 1930; Gamo, 1964; Cloude, 1986; Cloude and Pottier, 1996; 1997a). The largest eigenvalue indicates the dominant scattering, and the importance of one scattering compared to the others is measured with the target entropy, defined by Von Neumann (1955) as

$$H = - \sum_{i=1}^n P_i \log_n P_i \quad (60)$$

where P_i is the normalized eigenvalue $P_i = \lambda_i / \sum_{k=1}^n \lambda_k$, and n is the number of eigenvalues (Gamo, 1964; Mandel, 1963; Cloude, 1986; Cloude and Pottier, 1996). As pointed out in Gamo (1964), Cloude (1985), and Cloude and Pottier (1996; 1997a), target entropy is a measure of target disorder, with $H = 1$ for a completely random target for which all eigenvalues λ_i are equal, and $H = 0$ for a simple target (single scatterer). Target entropy is used to assess the dominance of a scattering vector (Cloude and Pottier, 1996; 1997a). If the entropy is low, then the system is considered weakly depolarizing and the dominant target scattering component is the eigenvector corresponding to the largest eigenvalue. If the entropy is high, the target is depolarizing and the full eigenvalue spectrum should be considered (Cloude and Pottier, 1996).

Under a reciprocal assumption, Cloude and Pottier (1996; 1997a) introduced the following parameterization of the eigenvector of the 3×3 target coherency matrix $[\mathbf{T}]$ in the target \vec{k} (Equation (31)) basis:

$$\vec{e} = [\cos \alpha, \sin \alpha \cos \beta \exp(j\delta), \sin \alpha \sin \beta \exp(j\gamma)]^T \quad (61)$$

where α is referred to as the scattering type (equivalent to the Kennaugh–Huynen depolarization angle in the case of pure scattering $H = 0$) and varies between 0° and 90° (0° for a trihedral, 45° for a dipole, and 90° for a dihedral); and β corresponds to the rotation of the scatterer axis about the LOS and is equivalent to the Kennaugh orientation angle in the case of pure scattering $H = 0$. The pair α/H has been used as the basis for the development of new classification methods introduced for analysis of polarimetric data (Lee et al., 1999a; Ferro-Famil et al., 2001). To remove the entropy ambiguity that might happen for scattering mechanisms with different eigenvalue distributions but with similar intermediate entropy values, the anisotropy A was introduced (Cloude, 1997; Cloude and Pottier, 1997b). This permits the development of a more effective classification (Pottier and Lee, 1999) based on $\alpha/H/A$.

The characteristic decomposition target covariance or coherency Hermitian positive semi-definite matrices permits an incoherent target decomposition, since it leads to a diagonalized matrix with positive real (noncomplex) eigenvalues (i.e., decomposition into a statistically independent set of target vectors with no phase information (Wiener, 1930; Tsang et al., 1985)). This confirms Wiener's (1930) definition of characteristic decomposition: "Hermitian matrix transformed into a diagonal matrix representing a set of completely incoherent phenomena in the orthonormal set of eigenvectors". In addition, the incoherent target decomposition can only be applied at low resolution scale. For an unbiased estimation of the ITCO Cloude and Pottier's parameters, the covariance and coherency matrices should be estimated over a sufficiently large window in which the scene and speckle signals are locally stationary and ergodic (Touzi et al., 1999). Consequently, high-resolution coherent Kennaugh–Huynen or SSCM target decomposition should be applied prior to the incoherent target decomposition. Incoherent target decomposition is then applied

in areas of noncoherent scattering, in which coherent target decomposition is meaningless (Touzi and Charbonneau, 2002). The tools introduced in Touzi and Charbonneau (2002) can be used for segmentation of the scene under study into a coherent class and an incoherent class, in which the CTD and the ICTD can be applied separately.

Speckle filtering of polarimetric SAR images

Speckle statistics

One-look polarimetric data are generally provided under the scattering matrix format. The complex signal backscattered from each resolution cell is characterized by the p -tuple scattering matrix vector \vec{x} of Equation (28), where $p = 4$ for the general case and $p = 3$ for a reciprocal medium ($S_{HV} = S_{VH}$). The statistics of \vec{x} were derived for the special case of a circular complex Gaussian process (Goodman, 1963; 1975). The probability density function (pdf) of \vec{x} was expressed as a function of its covariance matrix $\Sigma = E(\vec{x} \cdot \vec{x}^{*T})$ as

$$p(\vec{x} | \Sigma) = \frac{1}{\pi^p \cdot |\Sigma|} \cdot \exp(-\vec{x}^{*T} \cdot [\Sigma]^{-1} \cdot \vec{x}) \quad (62)$$

Multilook data might be characterized by the covariance sample $[C]$ of Equation (29), as seen in the section titled "Target covariance and target coherency matrices". The statistics of $[C]$ were derived in Goodman (1963) under the assumption of a zero mean p -variate complex circular Gaussian process. Its pdf is the Wishart distribution (Wishart, 1928) given by Goodman (1963):

$$p([C] | \Sigma) = \frac{L^p \cdot |C|^{L-p}}{\pi^{p(p-1)/2} \Gamma(L) \dots \Gamma(L-p+1) \cdot |\Sigma|^L} \times \exp(-L \cdot \text{Tr}[\Sigma]^{-1} \cdot [C]) \quad (63)$$

where $\text{Tr}(\Sigma)$ denotes the trace of the matrix Σ , and $|[C]|$ is the determinant of $[C]$.

It is worth noting that the statistics of Equations (62) and (63) were derived under the condition that the speckle p -tuple vector $\vec{x} = (x_1, \dots, x_p)^T$ is a zero mean complex circular Gaussian process. This supposes the following (Goodman, 1963; 1975): (i) each channel polarization, x_k for $k = 1, p$, is a zero mean complex circular Gaussian process channel, an assumption that is valid for a fully developed speckle (Tur et al., 1982; Goodman, 1975; Touzi, 2002); and (ii) the p channels are jointly circular complex Gaussian processes, meaning that the p zero mean complex circular Gaussian process should, in addition, be jointly Gaussian and satisfy the following conditions:

$$\begin{aligned} E(I_k I_l) &= E(Q_k Q_l) \\ E(I_k Q_l) &= -E(Q_k I_l) \end{aligned} \quad (64)$$

where I_k and Q_k are the real and imaginary parts, respectively, of x_k for $k = 1, p$.

Therefore, the speckle models of Equations (62) and (63) can only be applied in areas in which the previous conditions for a circular complex Gaussian process are satisfied. In particular, the conditions of Equation (64) that need a large sample size to be realized (Touzi et al., 1999) should be validated. This might limit the use of these models, and mainly the multilook Wishart model, to coarse-resolution SAR applications.

Speckle-scene model

Complex multiplicative speckle model

Fully developed speckle might be modeled as a multiplicative stationary independent zero mean complex circular Gaussian process that models the scene reflectivity (Raney, 1980; Touzi, 2002). Under the assumption that the bandwidth of the signal is small compared with that of the SAR linear filter, the complex voltage at the output of the system might be expressed as the product of the complex scene signal and speckle complex voltage as

$$o = n_c s \quad (65)$$

where n_c is the speckle process at the input of the SAR system convoluted by the SAR impulse function (Saleh and Rabbani, 1980). If the pixels impulse response correlation is removed (Kuan et al., 1985), n_c is a white process, and Equation (65) represents the so-called complex multiplicative speckle model (Touzi, 2002). Note that the speckle-scene signal product of Equation (65) is expressed in terms of a zero mean complex circular Gaussian speckle signal and the scene complex reflectivity, whereas the conventional "intensity" multiplicative model (Lee, 1980; Touzi, 2002) expresses the observed intensity signal as the product of the intensity of the speckle circular Gaussian process with the scene intensity signal.

The complex multiplicative model of Equation (65) can be extended to the vectorial form, as done in Goze and Lopes (1993) and Touzi and Lopes (1994). The measured scattering vector $\vec{O} = (O_{HH}, O_{HV}, O_{VH}, O_{VV})^T$ is expressed as the product of the scene reflectivity vector $\vec{S} = (S_{HH}, S_{HV}, S_{VH}, S_{VV})^T$ and a diagonal matrix $[N]$ as

$$\vec{O} = [N] \cdot \vec{S} \quad (66)$$

with $[N] = \text{Diag}(\vec{n}_c)$, where $\vec{n}_c = (n_{HH}, n_{HV}, n_{VH}, n_{VV})^T$ represents the four-channel complex speckle realization vector (Goze and Lopes, 1993; Touzi and Lopes, 1994). The fact that speckle is independent from the scene reflectivity signal permits derivation of the equivalent expression that relates the observed and scene reflectivity covariance matrices, $[W_O] = \langle \vec{O} \vec{O}^{*T} \rangle$ and $[W_S] = \langle \vec{S} \vec{S}^{*T} \rangle$, as a function of the speckle covariance matrix $[W_n] = \langle \vec{n}_c \vec{n}_c^{*T} \rangle$ (Goze and Lopes, 1993; Touzi and Lopes, 1994). This relation was expressed in terms of the vectorial form \vec{W}_O , \vec{W}_S , and \vec{W}_n of the covariance matrices as

$$\vec{W}_O = [\text{Diag}(\vec{W}_n)] \cdot \vec{W}_S \quad (67)$$

where $[\text{Diag}(\vec{W}_n)]$ is a $p \times p$ diagonal matrix whose diagonal is equal to \vec{W}_n (Touzi and Lopes, 1994). This model, referred to as the polarimetric multiplicative model, was used in Touzi and Lopes (1994) as the basis for the development of a polarimetric filter that is applied to the observed covariance matrix, and as such to the Mueller or Kennaugh matrices. The polarimetric multiplicative model (Equation (67)) also permits justifying in Touzi and Lopes that polarimetric speckle filtering should be completed in terms of speckle and observed signal covariance matrices, and not in terms of scattering matrices like that of Novak and Burl (1990), for preservation of the full polarimetric information.

Product model

The product model, referred to as the doubly stochastic model (Lewinski, 1983; Touzi, 2002), is currently used in conventional one-channel SAR imagery to represent nonstationary observed scene signals. Conditional speckle intensity is spatially averaged according to a speckle mean intensity pdf so as to provide an unconditional distribution of the observed intensity that is stationary in the mean. The same technique was applied in polarimetry in terms of observed, scene, and speckle covariance matrices (Yueh et al., 1989; 1991). Under the assumption that texture is independent of the channel polarization and that speckle is fully developed, Yueh et al. (1991) derived the following relationship for the observed covariance matrix (Joughin et al., 1994; Lopes and Sery, 1997; Oliver and Quegan, 1998):

$$[\mathbf{W}_O] = w \cdot [\mathbf{W}_h] = w \cdot [\mathbf{W}_n] \quad (68)$$

where w is the texture parameter defined in Novak and Burl (1990) and Yueh et al. (1991) as the ratio of the number m of scatterers per resolution cell to the average number of scatterers $\langle m \rangle$. $[\mathbf{W}_h]$, which was referred to as the covariance matrix for a homogeneous medium (Yueh et al., 1991; Joughin et al., 1994; Lopes and Sery, 1997), is in fact identical to the covariance matrix $[\mathbf{W}_n]$ of the zero mean complex circular Gaussian speckle process, as noted in Equation (68). The unconditional multivariate pdf of \vec{O} can then be written in terms of doubly stochastic model as

$$P(\vec{O}) = \int_0^{+\infty} P_N(\vec{O}|w \cdot [\mathbf{W}_n]) P_w(w(t)) dw(t), \quad (69)$$

where $P_N(\vec{O}|w \cdot [\mathbf{W}_n])$ is a multivariate Gaussian pdf of Equation (62) for (\vec{O}) with speckle covariance matrix $w \cdot [\mathbf{W}_n]$ (Novak and Burl, 1990; Yueh et al., 1991; Joughin et al., 1994).

The scalar product representation of Equation (68) separates the texture parameter w from the Wishart-distributed speckle covariance, and as result makes easier the derivation of observed statistics as a function of the texture a priori model P_w . If the scene texture w is gamma distributed, the integration of Equation (69) gives rise to a multivariate K distribution for the

observed intensity vector (\vec{O}) (Novak and Burl, 1990; Yueh et al., 1991).

For a multilook image, Equation (69) might be expressed in terms of covariance matrices, and the multivariate pdf of $[\mathbf{W}_O]$ can then be written in terms of a doubly stochastic model as

$$P([\mathbf{W}_O]) = \int_0^{+\infty} P_{\text{CovN}}([\mathbf{W}_O]|w \cdot [\mathbf{W}_n]) P_w(w(t)) dw(t) \quad (70)$$

where P_{CovN} is the Wishart distribution of Equation (63) (Joughin et al., 1994; Lee et al., 1994d; Lopes and Sery, 1997; Oliver and Quegan, 1998). Equation (69) was used in Lee et al. (1994d), Lopes and Sery (1997), and Oliver and Quegan (1998) to derive the multivariate K distribution of the observed covariance matrix for a gamma-distributed scene as a function of the number of looks of the image under study.

The product model of Equations (69) and (70) assumes that texture is independent of the polarization channel. Most of the authors have admitted that such an assumption is valid (Lopes and Sery, 1997; Oliver and Quegan, 1998). Sheen and Johnson (1992) and Joughin et al. (1994) showed experimentally, using polarimetric SAR data, that such a statement might not be true. Experimental tests completed within forested areas using polarimetric Convair-580 SAR data demonstrated the vulnerability of the product model (Beaulieu and Touzi, 1993; 2004). Analysis of the coefficient of variation on the HH, HV, and VV images revealed significant variations (5%–6%) of the texture measure with the polarization. The relatively high resolution (64 cm in azimuth per 5 m in range) of the Convair-580 SAR permits the demonstration that texture may depend on the polarization, as should be expected.

In summary, texture might be polarization dependent, and the validity of the product model should be assessed before the application of any speckle filtering or classification algorithm based on this model.

Principle of polarimetric speckle filtering

Speckle filtering remains mainly an estimation problem whose objective is to retrieve the scene reflectivity from the observed speckled SAR measurement. Such an estimation problem should be completed under stationarity and ergodicity signal conditions so as to provide a meaningful and accurate estimate of the scene signal (Touzi, 2002). Touzi and Lopes (1994) were the first to show that speckle filtering should not be conducted in terms of a scattering matrix. Speckle filtering should be solved in terms of a covariance matrix, which is then used to deduce the Kennaugh or Mueller matrix (Touzi and Lopes, 1994). The unspckled scene signal covariance should be extracted from the covariance of the observed signal estimated within a moving window in which the scene and speckle signals are stationary and ergodic (Touzi, 2002). The wave backscattered from the area covered by the processing window is generally a partially polarized wave and, as such, should be represented by the Kennaugh or Mueller matrix that is deduced from the filtered covariance matrix.

This principle of speckle filtering introduced in Touzi and Lopes (1994) enables certain filters to be eliminated, such as the Novak filter (Novak and Burl, 1990), which combines all scattering vector correlation information into a single quantity, the scattering matrix. This matrix is not adequate for representation of the filtered scene received wave, which should be partially polarized because of the spatial scene signal variations within the processing window (i.e., target coherence larger than measurement time, as seen in the section titled “One-look and multilook SAR data processing”). The Novak prewhitening filter might be used to facilitate image interpretation, but results obtained should be considered with caution because of the eventual loss of polarimetric information.

Product or multiplicative speckle model

Product model filtering

Lopes and Sery (1997) developed a filter based on the product model of Equations (68) and (70). Under the assumption that texture is gamma distributed, a maximum a posteriori (MAP) algorithm is derived for estimation of the local texture coefficient w . An iterative method is used to compute both the texture coefficient and speckle covariance estimate for a given processing window. Speckle was assumed to be nonstationary, in contrast to the filters in this section (Touzi and Lopes, 1994; Lee et al., 1999b). Unfortunately, this filter is of limited application because it has to be limited to areas in which the product model is valid and the scene signal is gamma distributed. This means that the filter can only be applied within areas in which texture is independent of polarization (i.e., product model’s assumption), and the texture coefficient w is gamma distributed. In addition, the results obtained with this filter should be used with caution because of the eventual presence of a bias related to the MAP estimate (Lopes and Sery, 1997; Touzi, 2002). This remark can also be said about the Schou and Skriver (2001) polarimetric annealing method filter, which should also be limited to homogeneous areas and textured areas with texture independent of polarization. Like the one-channel annealing MAP filter (McConnell et al., 1995; Oliver and Quegan, 1998), this two-level estimation filter suffers from a bias that depends on texture, as noted in Schou and Skriver. This bias, which is obtained at the first iteration of the annealing process, is due to the small number of independent samples being used to estimate second-level statistics (Touzi, 2002). Such a bias is not introduced by the one-level minimum mean square error (MMSE) filters (Touzi, 2002), which additionally are not limited by product model validity constraints.

Multiplicative speckle model filtering

All the polarimetric filters developed under speckle stationarity assumption are an extension of the Lee MMSE scalar filter (Lee, 1980) introduced in 1980 for one-channel polarization images. Lee et al. (1991) introduced a vectorial MMSE filter for speckle reduction of multipolarized SAR images. Using a tridimensional “intensity” multiplicative

model, Lee et al. derived the vectorial MMSE filter that provides an estimation of the intensity vector ($|S_{HH}|^2$, $|S_{HV}|^2$, $|S_{VV}|^2$) from the observed measured intensity. Goze and Lopes (1993) extended the study of Lee et al. to derive a nine-vectorial MMSE filter for one look image, which provides in addition to the three-channel unspeckled intensities the three double products of the complex scattering vector. Touzi and Lopes (1994) extended the Goze and Lopes one-look MMSE filter to multilook SAR data. The linear MMSE scene signal covariance vector was derived, under the target reciprocity assumption, as

$$\hat{X} = E(\bar{X}) + [\mathbf{Cov}(\bar{X})]E([\mathbf{V}]^T)[\mathbf{Cov}(\bar{Y})]^{-1} \cdot [\bar{Y} - E([\mathbf{V}])E(\bar{X})] \quad (71)$$

where \mathbf{Cov} denotes the covariance matrix, \bar{Y} is the 16-dimensional real vector equivalent to the 10-dimensional complex observed covariance vector \bar{W}_O , \bar{X} is the 16-dimensional real vector equivalent to the 10-dimensional complex scene vector \bar{W}_S , and $[\mathbf{V}]$ is the 16×16 real matrix representation of the 10×10 complex speckle covariance matrix $[\mathbf{Diag}(\bar{W}_n)]$ (Touzi and Lopes, 1994). The scene parameters involved in Equation (71) were derived from observed averaged local statistics. The multiplicative model of Equation (66) was used under the assumption that speckle noise (Touzi, 2002) is stationary and completely polarized. Such an assumption significantly simplifies filter processing, since speckle statistics that are constant on the scene need to be estimated only once. In addition, the speckle information related to the illuminated scenes, such as the degree of polarization of the scattered wave, is preserved on the filtered image (Touzi and Lopes, 1994; Touzi, 2002).

Unfortunately, even though the Touzi and Lopes (1994) filter appears solid in theory, it suffers in practice from some implementation problems, which are related to the difficulty in filtering the cross-product terms. These problems are currently being solved, and the results will be discussed in a future publication. Lee et al. (1999b) and Lee and Grues (2000) circumvented this problem in the so-called POLSAR filter by a simplification of the multidimensional MMSE to one dimension. The same linear MMSE derived for conventional one-channel SAR images (Lee, 1980) is used, and the scalar estimate is replaced by the covariance matrix as (Lee et al., 1999b; Lee and Grues, 2000)

$$\bar{W}_S = E(\bar{W}_S) + b \cdot [\bar{W}_O - E(\bar{W}_O)] \quad (72)$$

The weighting coefficient b is computed using the span image and is applied to all the elements of the covariance matrix according to Equation (72). For optimum application of the stationary MMSE filter within nonstationary conditions (Touzi, 2002), POLSAR is combined with edge detectors that are applied on the span image (Lee et al., 1999b).

The Lee POLSAR is currently the most used filter for speckle reduction of polarimetric SAR data. Recently, Lee et al. (2003) introduced an improved version of POLSAR that takes into account the scattering information provided by the

polarimetric information. Freeman and Durden (1998) target decomposition is first applied to segment the scene in three scattering categories: double bounce, surface, and volume scattering. A POLSAR estimate is then computed using only pixels that belong to the same scattering class. Combining scattering information with statistical information is a very interesting idea that should guide the future development of polarimetric speckle filters.

Classification of polarimetric SAR images

Since 1987, polarimetric SAR data classification has been an active field of research, and various methods for supervised and unsupervised classification have been published (Kong et al., 1987; Lim et al., 1989; Kong, 1990; Van Zyl, 1989; 1992; Rignot et al., 1992; Touzi et al., 1992a; Pottier and Cloude, 1995; Cloude and Pottier, 1997a; Freeman and Durden, 1998; Lee et al., 1999a; 2001; Lombardo and Oliver, 2002; Pottier and Lee, 1999; Ferro-Famil et al., 2001).

Supervised classification

Supervised classifications use training sets for each class that are selected based on ground-truth maps. Kong et al. (1987) were the first to introduce a supervised classification method for polarimetric images. They showed that polarimetric SAR data with the full amplitude and phase information of the scattered wave provide improved classification accuracy compared with any subset of the polarimetric data. The multivariate complex Gaussian distribution (Equation (62)) of the three complex polarimetric components, HH, HV, and VV, is used to derive the classification distance measure that optimizes the Bayes likelihood ratio test on one-look SAR data. The distance measure for the m th class ω_m is given by

$$d(\bar{\mathbf{x}}, \omega_m) = \bar{\mathbf{x}}^{*T} [\mathbf{C}_m]^{-1} \bar{\mathbf{x}} + \ln |\mathbf{C}_m| - \ln [P(\omega_m)] \quad (73)$$

where $[\mathbf{C}_m]$ is the covariance matrix of the class ω_m , $|\mathbf{C}_m|$ is the determinant of $[\mathbf{C}_m]$, and $P(\omega_m)$ is the a priori probability of class ω_m (Kong et al., 1987; Lim et al., 1989). The feature vector $\bar{\mathbf{x}}$ is assigned to class ω_m if $d(\bar{\mathbf{x}}, \omega_m) \leq d(\bar{\mathbf{x}}, \omega_j)$ for all $j \neq m$.

The probability of error for a two-class problem was calculated (Kong et al., 1987) using the expression derived by Fukunaga and Krile (1969) for multivariate Gaussian distributions. The pdf of various single measurements and their classification distance measure, as well as the corresponding probability of classification errors, were also derived. Monte Carlo simulations and polarimetric radar measurements (at 35 GHz) of forest and grass fields permit demonstrating that the fully polarimetric data yield a smaller probability of error than any of the errors obtained using the single features |HHI, |HVI, |VVI, |HH/VVI, |HV/|HHI, and $\phi_{HH} - \phi_{VV}$. This leads to the conclusion that full polarimetric results are optimal and provide better classification performance than single-feature measurements (Kong et al., 1987). This result was confirmed by Lim et al.

(1989) using L-band AirSAR data, and the normalized Bayes classifier (Yueh et al., 1989; Lim et al., 1989) was applied to circumvent possible absolute calibration problems. These supervised classifications are generally applied under the assumption of equal a priori probabilities for all classes. Improvement of the normalized Bayes classifier (Yueh et al., 1989; Lim et al., 1989) performance was completed in Van Zyl (1992) using a classification with various a priori class probabilities. Van Zyl classification uses an iterative process for an optimum matching of the various a priori probabilities of the scene classes.

The aforementioned maximum likelihood (ML) (Kong et al., 1987) and normalized ML (Yueh et al., 1989; Lim et al., 1989) classifiers, however, are only limited to one-look polarimetric SAR data. Using the covariance Wishart distribution of Equation (63), Lee et al. (1994b) extended the ML classifier of Kong et al. (1987) to multilook data. The classification distance is given for an L -look image by

$$d([\mathbf{C}], \omega_m) = L[\ln |\mathbf{C}_m| + \text{Tr}([\mathbf{C}_m]^{-1} [\mathbf{C}])] - \ln [P(\omega_m)] \quad (74)$$

where $[\mathbf{C}]$ is the observed covariance matrix sample of Equation (29), $[\mathbf{C}_m]$ is the covariance matrix of the class ω_m , and $P(\omega_m)$ is the a priori probability of class ω_m (Lee et al., 1994b). The feature covariance $[\mathbf{C}]$ is assigned to the class ω_m if the distance is the smallest. A special case of the L -look ML classification distance of Equation (74) is the Kong et al. (1987) one-look classification distance of Equation (73).

It is worth noting that the a priori class probability $P(\omega_m)$ becomes less significant with an increase in the number of looks, according to Equation (74). Under the assumption that $P(\omega_m)$ is the same for all the classes, the distance measure becomes independent of the number of looks L . Lee et al. (1999a; 2001) and Lee and Grues (2000) used this argument to apply the distance measure after application of POLSAR speckle filtering. This would assume that the filtered image includes a constant number of looks (independent samples) per pixel in the whole image. Such an assumption might not hold at the proximity of edges, where a smaller window is used using edge-detection techniques for an accurate filter parameter estimation (Lee et al., 1999b), and the classification of these pixels should be considered with care.

The use of additional scene a priori information in the context of a MAP classifier should improve the classification, as shown in Rignot et al. (1992) for the one-look ML classifier. Rignot et al. showed that the results obtained using a MAP classifier improves classification accuracy by 10%–20% compared with the ML classifier, which assumes equal a priori probabilities for the classes and no spatial correlation between the polarimetric measurements.

Unsupervised classification

Unsupervised classification classifies the image automatically by finding clusters based on a certain criterion. The tight relation between natural media physical properties and their

polarimetric features leads to highly descriptive classification results that can be interpreted by analyzing underlying scattering mechanisms (Van Zyl, 1989; Touzi et al., 1992a; Cloude and Pottier, 1997a; Freeman and Durden, 1998; Lee et al., 1999b; 2001; Pottier et al., 1999; Ferro-Famil et al., 2001).

Van Zyl (1989) was the first to introduce an unsupervised classification based on polarization properties of each pixel of the image being analyzed. The relationship between the orientation angle and handedness of the transmit polarization to the corresponding parameters of the received wave is assessed for each pixel and is then assigned to one of the three simple classes: odd number of reflections class, even number of reflections class, and diffuse scattering. Illustration of this classification is presented in Evans et al. (1988) and Van Zyl (1989) using the San Francisco AirSAR image.

Touzi et al. (1992a) introduced an unsupervised classification based on the bidimensional scattered wave information provided by the maximum degree of polarization p_{\max} and the dynamic range of variation of the degree of polarization $\delta p = p_{\max} - p_{\min}$. The maximum degree of polarization p_{\max} was used to characterize the type of scattering mechanism, whereas δp provided information related to the complexity of the scattering (Touzi et al., 1992a). An illustration of the method using the San Francisco AirSAR image demonstrated a high potential of the bidimensional scattering classification (Touzi et al., 1992a).

Cloude and Pottier (1997b; 1997a) and Pottier and Cloude (1995) introduced an unsupervised classification based on Cloude's target decomposition theory (Cloude, 1985; Cloude and Pottier, 1996). The incoherent target decomposition permits the derivation of a two-dimensional H/α classification plane, where all random scattering mechanisms can be represented (Pottier et al., 1999). The H/α plane is subdivided into eight basic zones characteristic of different scattering behaviors, and the different class boundaries have been determined so as to discriminate surface scattering, volume diffusion, and double-bounce scattering along the α axis and low, medium, and high degrees of randomness along the entropy axis (Cloude and Pottier, 1997a; Pottier et al., 1999). The two-dimensional H/α classification was improved in Cloude and Pottier (1997b) and Pottier et al. (1999) using the additional information provided by the anisotropy A (Cloude, 1997; Cloude and Pottier, 1997b), which is particularly useful for discriminating scattering mechanisms with different eigenvalue distributions but with similar intermediate entropy values (Cloude, 1986; Cloude and Pottier, 1997b; Pottier et al., 1999).

Freeman and Durden (1998) introduced an unsupervised classification based on a three-component scattering model they developed. The components of the scattering matrix are analyzed to assign each pixel to one of three scattering categories: first-order bragg surface, double-bounce scattering, and volume scattering. The method, which was validated successfully using AirSAR data (Freeman and Durden, 1998), was recently integrated in speckle filtering (Lee et al., 2003) and classification (Lee et al., 2002b; 2004) algorithms, resulting in improved performances.

Combination of supervised and unsupervised classifications

Combination of the unsupervised and supervised classification techniques appears to be very promising, as shown in Lee et al. (1999a; 2002b). Lee et al. (1999a) introduced a combination of the H/α classification with their supervised Wishart ML classifier (Lee et al., 1994b) of Equation (74). The H/α classification is first applied to form training sets as input for the ML classifier of Equation (74). The classified results are then used as training sets for the next iteration using the ML classifier method. Significant improvement in each iteration has been observed. The iteration ends when the number of pixels switching classes becomes smaller than a predetermined number, or when other termination criteria are met. This method was successfully applied for ice classification in Scheuchl et al. (2003). Lee et al. (2002b) also introduced a combination of the Freeman and Durden (1998) unsupervised classification with the Wishart ML classifier of Equation (74), which leads to interesting results (Lee et al., 2002b; 2003).

All of the aforementioned methods currently used for classification of polarimetric SAR images are based on multivariate complex Gaussian or Wishart models. Such distributions may not be suitable for textured areas, and the classification based on these models might be less effective when texture is present. Texture models such as the multivariate K -distribution model, which was derived using the product model for a gamma-distributed scene (Lee et al., 1994d; Lopes and Sery, 1997), as discussed in the section titled "Product model", might be integrated in the classification process for better performance. The integration of the K model in the ML likelihood segmentation technique of Beaulieu and Touzi (2004) improves the results compared with those from the Wishart and Gaussian model based segmentation, as shown in Beaulieu and Touzi.

Conclusion

With all the upcoming satellite polarimetric SARs, such as RADARSAT-2, ALOS-PALSAR, and TerraSARs, radar polarimetry will start a new era with a wider set of available polarimetric SAR data in X-, C-, and L-bands. The potential of polarization information for target characterization depends strongly on the tools used for information extraction. The parameters of scattered and received partially polarized waves that were mainly used in the 1990s (Evans et al., 1988; Kostinski and Boerner, 1988; Van Zyl et al., 1987b; Touzi et al., 1992a) should still be investigated as potential sources of information, in addition to the parameters issued from incoherent target decomposition theory (Cloude and Pottier, 1997a). High-resolution SAR coherent target decomposition should be applied prior to incoherent target decomposition within areas in which the coherent nature of the scattering is validated (Touzi and Charbonneau, 2002). The large window size required for an accurate estimation of target covariance and

coherency matrices might limit the incoherent target decomposition to coarse-resolution applications. Speckle-scene modeling needs more investigation. The product model currently in use is only limited to texture that is independent of polarization, and a more general model that takes into account polarization texture dependence is needed. This would permit the development of more effective tools for polarimetric speckle filtering and image classification and segmentation. Further theoretical and experimental investigations using airborne and satellite polarimetric SAR data and scatterometer measurements are needed for a better comprehension of the physical meaning of the various target and backscattered wave parameters. This would suppose that the polarimetric satellite SAR data, which will soon be extensively available, are well calibrated for meaningful polarization information extraction.

Acknowledgements

The authors would like to thank the anonymous reviewers for their helpful comments and suggestions.

References

- Agrawal, A.B., and Boerner, W.-M. 1989. Redevelopment of Kennaugh's target characteristic polarization state theory using the polarization transformation ratio formalism for the coherent case. *IEEE Transactions on Geoscience and Remote Sensing*, Vol. 27, No. 1, pp. 2–14.
- Ainsworth, T.L., Jansen, R.W., Lee, J.S., and Fiedler, R. 1999. Sub-aperture analysis of high-resolution polarimetric SAR data. In *IGARSS'99, Proceedings of the International Geoscience and Remote Sensing Symposium*, June 1999, Hamburg, Germany. IEEE, New York.
- Antar, Y.M.M., Hendry, A., and McCormick, G.C. 1992. Circular polarization for remote sensing of precipitation. *IEEE Transactions on Antennas and Propagation*, Vol. 34, No. 6, pp. 7–16.
- Azzam, R.M.A. 1977. *Ellipsometry and polarized light*. North-Holland Publishing Co., Amsterdam, The Netherlands.
- Barakat, R. 1981. Bilinear constraints between elements of the 4x4 Mueller-Jones transfer matrix of polarization theory. *Optics Communications*, Vol. 38, pp. 159–161.
- Barakat, R. 1985. The statistical properties of partially polarized waves. *Journal of the Optical Society of America*, Vol. 32, No. 3, pp. 295–312.
- Barnes, R.M. 1986. Antenna polarization calibration using in-scene reflectors. In *Proceedings of the 10th DARPA/Tri-Service Millimeter Wave Symposium*. U.S. Army Harry Diamond Laboratory, Adelphi, Md.
- Beaulieu, J.M., and Touzi, R. 1993. Segmentation of textured scenes using polarimetric SARs. *IEEE Transactions on Geoscience and Remote Sensing*. Submitted.
- Beaulieu, J.M., and Touzi, R. 2004. Segmentation of textured scenes using polarimetric SARs. *IEEE Transactions on Geoscience and Remote Sensing*. In press.
- Boerner, W.M., and Xi, A.-Q. 1990. Characteristic radar target polarization state theory for the coherent monostatic and reciprocal case using the generalized polarization transformation ratio formulation. *AEU*, Vol. 44, No. 4, pp. 273–281.
- Boerner, W.M., El-Arini, M.B., Chan, C.-Y., and Matoris, P.M. 1981. Polarization dependence in electromagnetic inverse problems. *IEEE Transactions on Antennas and Propagation*, Vol. AP-29, pp. 262–271.
- Boerner, W.M., Yan, W.-L., Xi, A.-Q., and Yamaguchi, Y. 1991. On the principles of radar polarimetry (invited review): the target characteristic polarization state theory of Kennaugh, Huynen's polarization fork concept, and its extension to the partially polarized case. *IEEE Proceedings, Special Issue on Electromagnetic Theory*, Vol. 79, No. 10, pp. 1538–1550.
- Boerner, W.M., Walther, M., and Segal, A.C. 1993a. Development of the polarimetric contrast enhancement optimization procedure and its application to sea surface scatter in POLSAR image analysis. In *IGARSS'93, Proceedings of the International Geoscience and Remote Sensing Symposium*, 18–21 Aug. 1993, Tokyo, Japan. IEEE, New York.
- Boerner, W.M., Liu, C., and Zhang, L. 1993b. Comparison of the optimization procedures for the 2x2 Sinclair and 4x4 Mueller matrices in coherent polarimetry and its application to radar target versus background clutter discrimination in microwave sensing and imaging. *International Journal of Advances in Remote Sensing (IJARS)*, Vol. 2, No. 1-1, pp. 55–82.
- Boerner, W.M., Mott, H., Lüneburg, E., Livingstone, C., Brisco, B., Brown, R.J., Paterson, J.S., Cloude, S.R., Krogager, E., Lee, J.S., Schuler, D.L., Van Zyl, J.J., Randall, D., Budkewitsch, P., and Pottier, E. 1998. Polarimetry in radar remote sensing: basic and applied concepts. In *Manual of remote sensing: principles and applications of imaging radar*. Edited by R.A. Ryerson. John Wiley & Sons, Inc., New York. Vol. 3, No. 5, pp. 271–356.
- Borgeaud, M., Shin, R.T., and Kong, J.A. 1987. Theoretical models for polarimetric radar clutter. *Journal of Electromagnetic Waves and Applications*, Vol. 1, No. 1, pp. 73–89.
- Born, M., and Wolf, E. 1959. *Principles of optics: electromagnetic theory of propagation, interference and diffraction of light*. Pergamon Press, Elmsford, N.Y.
- Cameron, W.L., Youssef, N., and Leung, L.K. 1996. Simulated polarimetric signatures of primitive geometrical shapes. *IEEE Transactions on Geoscience and Remote Sensing*, Vol. 34, No. 3, pp. 793–803.
- Chandrasekhar, S. 1960. *Radiative transfer*. Dover, New York.
- Christensen, E.L., Skou, N., Dall, J., Woelders, K.W., Jorgensen, J.H., Granholm, J., and Madsen, S.N. 1998. EMISAR absolutely calibrated polarimetric L- and C-band SAR. *IEEE Transactions on Geoscience and Remote Sensing*, Vol. 6, pp. 1852–1855.
- Cloude, S.R. 1985. Radar target decomposition theorems. *Electronics Letters*, Vol. 21, No. 1, pp. 22–24.
- Cloude, S.R. 1986. Group theory and polarization algebra. *Optik*, Vol. 75, No. 1, pp. 26–36.
- Cloude, S.R. 1992. Uniqueness of target decomposition theorems in radar polarimetry. In *Proceedings of the NATO Advanced Research Workshop on Direct and Inverse Methods in Radar Polarimetry*. Edited by W.-M. Boerner et al. September 1988. Kluwer Academic Publishers, Dordrecht, The Netherlands. NATO ASI Series, Series C: Mathematical and Physical Sciences, Vol. 350, pp. 267–296.
- Cloude, S.R. 1997. Wide band polarimetric radar inversion studies using the entropy-alpha decomposition. In *Wideband interferometric sensing and imaging polarimetry*. Edited by H. Mott and W.M. Boerner. International Society for Optical Engineering, Bellingham, Wash. Proceedings of SPIE, Vol. 3120, pp. 118–129.

- Cloude, S.R., and Papathanassiou, K.P. 1998. Polarimetric SAR interferometry. *IEEE Transactions on Geoscience and Remote Sensing*, Vol. 36, pp. 1551–1565.
- Cloude, S.R., and Pottier, E. 1996. A review of target decomposition theorems in radar polarimetry. *IEEE Transactions on Geoscience and Remote Sensing*, Vol. 34, No. 2, pp. 498–518.
- Cloude, S.R., and Pottier, E. 1997a. An entropy based classification scheme for land applications of polarimetric SARs. *IEEE Transactions on Geoscience and Remote Sensing*, Vol. 35, No. 2, pp. 68–78.
- Cloude, S.R., and Pottier, E. 1997b. Application of the H/A/ α polarimetric decomposition theorem for land classification. In *Wideband interferometric sensing and imaging polarimetry*. Edited by H. Mott and W.M. Boerner. International Society for Optical Engineering, Bellingham, Wash. Proceedings of SPIE, Vol. 3120, pp. 132–143.
- Conradsen, K., Nielsen, A.A., Schou, J., and Skriver, H. 2003. A test statistic in the complex Wishart distribution and its application to change detection in polarimetric SAR data. *IEEE Transactions on Geoscience and Remote Sensing*, Vol. 41, No. 1, pp. 4–19.
- Corr, D.G., and Rodrigues, A.F. 2002. Alternative basis matrices for polarimetric decomposition. In *EUSAR 2002, Proceedings of the 4th European Union Conference on Synthetic Aperture Radar*, 4–6 June 2002, Cologne, Germany.
- Curlander, J.C., and McDonough, R.N. 1991. *Synthetic aperture radar: system and signal processing*. John Wiley & Sons, Inc., New York.
- Davidovitz, M., and Boerner, W.-M. 1986. Extension of Kennaugh's optimal polarization concept to the asymmetric matrix case. *IEEE Transactions on Antennas and Propagation*, Vol. 34, No. 4, pp. 569–574.
- Deschamps, G.A. 1951. Geometrical representation of the polarization of a plane electromagnetic wave. *Proceedings of the IRE*, Vol. 39, pp. 540–544.
- Deschamps, G.A., and Mast, P.E. 1973. Poincaré sphere representation of partially polarized. *IEEE Transactions on Antennas and Propagation*, Vol. AP-21, No. 4, pp. 474–478.
- Dubois, P.C. 1992. Approach to derivation of SIR-C science requirements. *IEEE Transactions on Geoscience and Remote Sensing*, Vol. 30, pp. 1145–1148.
- Dubois, P.C., and Norikane, L. 1987. Data volume reduction for imaging radar polarimetry. In *IGARSS'87, Proceedings of the International Geoscience and Remote Sensing Symposium*, 18–21 May 1987, Ann Arbor, Mich. IEEE, New York. pp. 691–697.
- Dubois-Fernandez, P., Ruault du Plessis, O., Vaizan, B., Dupuis, X., Cantalloube, H., Coulombeix, C., Titin-Schnaider, C., Dreuillet, P., Boutry, J.M., Canny, J.P., Peyret, J., Martineau, P., Chanteclerc, M., and Bruyant, J.P. 2002. The ONERA RAMSES SAR system. In *IGARSS'02, Proceedings of the International Geoscience and Remote Sensing Symposium*, 24–28 June 2002, Toronto, Ont. IEEE, New York.
- Engen, G., and Johnson, H. 1995. SAR-ocean wave inversion using image cross spectra. *IEEE Transactions on Geoscience and Remote Sensing*, Vol. 33, No. 4, pp. 1044–1056.
- Eom, H.J., and Boerner, W.M. 1991. Statistical properties of phase difference between two orthogonally-polarized SAR signals. *IEEE Transactions on Geoscience and Remote Sensing*, Vol. 29, No. 11, pp. 182–184.
- Evans, D.L., Farr, T.G., Van Zyl, J.J., and Zebker, H.A. 1988. Radar polarimetry: analysis tools and applications. *IEEE Transactions on Geoscience and Remote Sensing*, Vol. 26, No. 6, pp. 774–789.
- Ferro-Famil, L., Pottier, E., and Lee, J.S. 2001. Unsupervised classification of multifrequency and fully polarimetric SAR images based on the H/A/Alpha-Wishart classifier. *IEEE Transactions on Geoscience and Remote Sensing*, Vol. 39, No. 11, pp. 2332–2342.
- Ferro-Famil, L., Reigber, A., Pottier, E., and Boerner, W.M. 2003. Scene characterization using sub-aperture polarimetric SAR data analysis. *IEEE Transactions on Geoscience and Remote Sensing*, Vol. 41, No. 10, pp. 2264–2276.
- Foo, B.Y., Chaudhuri, S.K., and Boerner, W.M. 1984. A high frequency inverse scattering model to recover the specular point curvature from polarimetric scattering matrix data. *IEEE Transactions on Antennas and Propagation*, Vol. 32, No. 11, pp. 1174–1178.
- Foo, B.Y., Chaudhuri, S.K., and Boerner, W.M. 1990. Polarization correction and extension of the Kennaugh-Cosgriff target-ramp response equation to the bistatic case and applications to electromagnetic inverse scattering. *IEEE Transactions on Antennas and Propagation*, Vol. 38, No. 7, pp. 964–972.
- Freeman, A. 1991. A new system model for radar polarimeters. *IEEE Transactions on Geoscience and Remote Sensing*, Vol. 29, No. 4, pp. 761–767.
- Freeman, A. 1992. SAR calibration: an overview. *IEEE Transactions on Geoscience and Remote Sensing*, Vol. 30, No. 6, pp. 1107–1122.
- Freeman, A. 1995. SIR-C/X data quality and calibration results. *IEEE Transactions on Geoscience and Remote Sensing*, Vol. 33, No. 4, pp. 848–857.
- Freeman, A. 2003. Lessons learned from SIR-C calibration. In *ASAR/CEOS'2003, Proceedings of the Advanced SAR Workshop*, 24–27 June 2003, Montréal, Que. Canadian Space Agency, St. Hubert, Que.
- Freeman, A. 2004. Calibration of linearly polarized SAR data subject to Faraday rotation. *IEEE Transactions on Geoscience and Remote Sensing*. In press.
- Freeman, A., and Durden, S.L. 1998. A three-component scattering model for polarimetric SAR data. *IEEE Transactions on Geoscience and Remote Sensing*, Vol. 36, No. 3, pp. 963–973.
- Freeman, A., and Saatchi, S. 2004. On the detection of Faraday rotation in linearly polarized L-band SAR backscatter signatures. *IEEE Transactions on Geoscience and Remote Sensing*. In press.
- Freeman, A., Van Zyl, J.J., Klein, J.D., Zebker, H.A., and Shen, Y. 1992. Calibration of Stokes and scattering matrix format polarimetric SAR data. *IEEE Transactions on Geoscience and Remote Sensing*, Vol. 30, No. 3, pp. 531–539.
- Freeman, A., Villasenor, J., Klein, J.D., Hoogeboom, P., and Groot, J. 2001. On the use of multi-frequency and polarimetric radar backscatter features for classification of agricultural crops. *International Journal of Remote Sensing*, Vol. 15, No. 9, pp. 1799–1812.
- Fukunaga, K., and Krile, T.F. 1969. Calculation of Bayes recognition error for two multivariate Gaussian distributions. *IEEE Transactions on Computers*, Vol. C-18, No. 3, pp. 220–229.
- Gamo, H. 1964. Matrix treatment of partial coherence. In *Progress in optics*. Edited by E. Wolf. John Wiley and Sons, Inc., New York. Vol. 3, pp. 187–333.
- Giuli, D. 1986. Polarization diversity in radars. *Proceedings of the IEEE*, Vol. 74, No. 2, pp. 245–269.

- Goodman, J.W. 1963. Statistical analysis based on a certain multivariate complex Gaussian distribution: an introduction. *Annals of Mathematical Statistics*, Vol. 34, No. 152, pp. 152–180.
- Goodman, J.W. 1975. Statistical properties of laser speckle patterns. In *Laser speckle and related phenomena*. Edited by J.C. Dainty. Springer-Verlag, New York. pp. 10–75.
- Goodman, J.W. 1985. *Statistical optics*. John Wiley and Sons Inc., New York.
- Goze, S., and Lopes, A. 1993. A MMSE speckle filter for full resolution SAR polarimetric data. *Journal of Electromagnetic Waves and Applications*, Vol. 7, No. 5, pp. 293–305.
- Graves, C.D. 1956. Radar polarization power scattering matrix. *Proceedings of the IRE*, Vol. 44, pp. 248–256.
- Gray, A.L., Vachon, P.W., Livingstone, C.E., and Lukowski, T.I. 1990. Synthetic aperture radar calibration using reference reflectors. *IEEE Transactions on Geoscience and Remote Sensing*, Vol. 28, pp. 374–383.
- Greidanus, H., Hoozeboom, P., Koomen, P., Snoeij, P., and Pouwels, H. 1996. First results and status of the PHARUS phased array airborne SAR. In *IGARSS'96, Proceedings of the International Geoscience and Remote Sensing Symposium*, 27–31 May 1996, Lincoln, Nebr. IEEE, New York. pp. 1633–1635.
- Guissard, A. 1994. Mueller and Kennaugh matrices in radar polarimetry. *IEEE Transactions on Geoscience and Remote Sensing*, Vol. 32, No. 3, pp. 590–597.
- Hagfors, T.A. 1967. Study of the depolarization of lunar echoes. *Radio Science*, Vol. 2, pp. 445–465.
- Hawkins, R.H. 1990. Determination of antenna elevation pattern for airborne SAR using the rough target approach. *IEEE Transactions on Geoscience and Remote Sensing*, Vol. 28, No. 5, pp. 896–905.
- Hawkins, R.K., Touzi, R., Wind, A., Murnaghan, K., and Livingstone, C.E. 1999. Polarimetric calibration results and error budget for SAR-580 systems. In *Proceedings of the CEOS'99 Workshop*, 26–29 Oct. 1999, Toulouse, France. ESA Publications Division, Noordwijk, The Netherlands, ESA SP-450. Available from <http://www.estec.esa.nl/CONFANNOUN/99b02>.
- Hong, Y., and Horn, R. 1988. A canonical form for matrices under consimilarity. *Linear Algebra and its Applications*, Vol. 102, pp. 143–168.
- Horn, R. 1996. The DLR airborne SAR project E-SAR. In *IGARSS'96, Proceedings of the International Geoscience and Remote Sensing Symposium*, 27–31 May 1996, Lincoln, Nebr. IEEE, New York. pp. 1624–1628.
- Horn, R., Werner, M., and Mayr, B. 1990. Extension of the DLR airborne SAR system. In *IGARSS'90, Proceedings of the International Geoscience and Remote Sensing Symposium*, 20–24 May 1990, College Park, Md. IEEE, New York.
- Howell, B.J. 1979. Measurement of the polarization effects of an instrument using partially polarized light. *Journal of Mathematical Physics*, Vol. 10, pp. 809–812.
- Huynen, J.R. 1965. Measurement of the target scattering matrix. *Proceedings of the IEEE*, Vol. 53, No. 8, pp. 936–946.
- Huynen, J.R. 1970. *Phenomenological theory of radar targets*. Technical Report, University of Technology, Delft, The Netherlands.
- IEEE. 1983. IEEE standard definitions of terms for antennas. *IEEE Transactions on Antennas and Propagation*, Vol. AP-31, No. 6, pp. 11–26.
- Ionnidis, G.A., and Hammers, D.E. 1979. Optimum antenna polarizations for target discrimination in clutter. *IEEE Transactions on Antennas and Propagation*, Vol. AP-27, pp. 357–363.
- Ito, N., Hamazaki, T., and Tomioka, K. 2001. ALOS/PALSAR characteristics and status. In *Proceedings of the CEOS SAR Workshop 2001*, 2–5 April 2001, Tokyo, Japan. National Space Development Agency of Japan (NASDA), Tokyo. pp. 191–194.
- Jones, R.C. 1941. A new calculus for the treatment of optical systems: description and discussion of the calculus. *Journal of the Optical Society of America*, Vol. 31, pp. 488–493.
- Jones, R.C. 1947. A new calculus for the treatment of optical systems: a more general formulation and description of another calculus. *Journal of the Optical Society of America*, Vol. 37, No. 2, pp. 107–110.
- Jordan, R.L., Huneycutt, B.L., and Werner, M. 1995. The SIR-C/X SAR synthetic aperture radar system. *IEEE Transactions on Geoscience and Remote Sensing*, Vol. 33, No. 4, pp. 829–839.
- Joughin, I.R., Winebrenner, D.P., and Percival, D.B. 1994. Probability density functions for multi-look polarimetric signatures. *IEEE Transactions on Geoscience and Remote Sensing*, Vol. 32, No. 3, pp. 562–574.
- Kennaugh, K. 1951. *Effects of type of polarization on echo characteristics*. Antenna Laboratory, The Ohio State University, Columbus, Ohio. Technical Report OH 389-4, 35 pp., and OH 381-9, 39 pp.
- Kennaugh, K. 1952. Polarization properties of radar reflections. M.Sc. thesis, The Ohio State University, Columbus, Ohio.
- Kim, K., Mandel, L., and Wolf, E. 1987. Relationship between Jones and Mueller matrices for random media. *Journal of the Optical Society of America*, Vol. 4, No. 3, pp. 433–437.
- Klein, J.D. 1992. Calibration of complex polarimetric SAR imagery using backscatter correlations. *IEEE Transactions on Aerospace and Electronic Systems*, Vol. 28, pp. 183–194.
- Ko, H.G. 1962. On the reception of quasi-monochromatic partially polarized radio waves. *Proceedings of the IRE*, Vol. 50, pp. 1950–1957.
- Kong, J.A. (Editor). 1990. *Polarimetric remote sensing*. Elsevier Science Publishing Co., New York. Progress in Electromagnetics Research (PIER), Vol. 3.
- Kong, J.A., Swartz, A.S., Yueh, H.A., Novak, L.M., and Shin, R.T. 1987. Identification of terrain cover using the optimum polarimeter classifier. *Journal of Electromagnetic Waves and Applications*, Vol. 2, No. 2, pp. 171–194.
- Kostinski, A.B., and Boerner, W.M. 1986. On foundation of radar polarimetry. *IEEE Transactions on Antennas and Propagation*, Vol. 34, No. 12, pp. 1395–1404.
- Kostinski, A.B., and Boerner, W.M. 1987. On the polarimetric contrast optimization. *IEEE Transactions on Antennas and Propagation*, Vol. 35, No. 8, pp. 988–991.
- Kostinski, A.B., and Boerner, W.M. 1988. Optimal reception of partially polarized waves. *Journal of the Optical Society of America*, Vol. 5, No. 1, pp. 58–64.
- Kozma, A.E., Nichols, A.D., Rawson, R.F., Shackman, S.J., Haney, C.W., and Shanne, J.J. 1986. Multi-frequency, -polarization SAR for remote sensing. In *IGARSS'86, Proceedings of the International Geoscience and Remote Sensing Symposium*, Zurich, Switzerland. ESA Publications Division, Noordwijk, The Netherlands. ESA Publication SP-254, pp. 715–719.

- Krogager, E. 1990. New decomposition of the radar target scattering matrix. *Electronic Letters*, Vol. 26, No. 18, pp. 1525–1527.
- Kuan, D.T., Sawchuk, A.A., Strand, T.C., and Chavel, P. 1985. Adaptive noise smoothing filter for images with signal-dependent noise. *IEEE Transactions on Pattern Analysis and Machine Intelligence*, Vol. 2, pp. 165–177.
- Lee, J.S. 1980. Digital image enhancement and noise filtering by use of local statistics. *IEEE Transactions on Pattern Analysis and Machine Intelligence*, Vol. 2, pp. 165–168.
- Lee, J.S. 1981. Refined filtering of image noise using local statistics. *Computer Graphics and Image Processing*, Vol. 15, pp. 380–389.
- Lee, J.S., and Grues, M.R. 2000. Polarimetric SAR speckle filtering and terrain classification — an overview. In *Information processing for remote sensing*. Edited by C.H. Chen. World Scientific Publishing Co., Singapore. pp. 113–138.
- Lee, J.S., Grues, M.R., and Mango, S.A. 1991. Speckle reduction in multipolarization, multifrequency SAR imagery. *IEEE Transactions on Geoscience and Remote Sensing*, Vol. 29, No. 4, pp. 535–544.
- Lee, J.S., Hoppel, K.W., Mango, S.A., and Miller, A.R. 1994a. Intensity and phase statistics of multi-look polarimetric and interferometric SAR imagery. *IEEE Transactions on Geoscience and Remote Sensing*, Vol. 32, No. 5, pp. 1017–1028.
- Lee, J.S., Grues, M.R., and Kwok, R. 1994b. Classification of multi-look polarimetric SAR imagery based on complex Wishart distribution. *International Journal of Remote Sensing*, Vol. 15, pp. 2299–2311.
- Lee, J.S., Jurkevich, I., Dewaele, P., Wambacq, P., and Costerlinck, A. 1994a. Speckle filtering of synthetic aperture radar images: a review. *Remote Sensing Reviews*, Vol. 8, pp. 311–340.
- Lee, J.S., Schuler, D.L., Lang, R.H., and Ranson, K.J. 1994d. K-distribution for multi-look processed polarimetric SAR imagery. In *IGARSS'94, Proceedings of the 1994 International Geoscience and Remote Sensing Symposium*, 8–12 Aug. 1994, Pasadena, Calif. IEEE, New York. pp. 2179–2181.
- Lee, J.S., Grues, M.R., Ainsworth, T.L., Du, L., Schuler, D.L., and Cloude, S.R. 1999a. Unsupervised classification of polarimetric SAR images by applying target decomposition and complex Wishart distribution. *IEEE Transactions on Geoscience and Remote Sensing*, Vol. 37, No. 5, pp. 2249–2258.
- Lee, J.S., Grues, M.R., and de Grandi, G. 1999b. Polarimetric SAR speckle filtering and its implication for classification. *IEEE Transactions on Geoscience and Remote Sensing*, Vol. 37, No. 5, pp. 2363–2373.
- Lee, J.S., Schuler, D.L., and Ainsworth, T.L. 2000. Polarimetric SAR data compensation for terrain azimuth slope variation. *IEEE Transactions on Geoscience and Remote Sensing*, Vol. 38, No. 5, pp. 2153–2163.
- Lee, J.S., Grues, M.R., and Pottier, E. 2001. Quantitative comparison of classification capability: fully polarimetric versus dual- and single-polarization SAR. *IEEE Transactions on Geoscience and Remote Sensing*, Vol. 39, No. 11, pp. 2343–2351.
- Lee, J.S., Schuler, D.L., Ainsworth, D.L., Krogager, E., Kasilingam, D., and Boerner, W.M. 2002a. On the estimation of radar polarization orientation shifts induced by terrain slopes. *IEEE Transactions on Geoscience and Remote Sensing*, Vol. 40, pp. 30–41.
- Lee, J.S., Grues, M.R., Pottier, E., and Ferro-Famil, L. 2002b. Segmentation of polarimetric SAR images that preserves scattering mechanisms. In *EUSAR 2002, Proceedings of the 4th European Union Conference on Synthetic Aperture Radar*, 4–6 June 2002, Cologne, Germany.
- Lee, J.S., Grues, M.R., Ainsworth, D.L., Schuler, D.L., and Cloude, S.R. 2003. Coherence estimation and speckle filtering based on scattering properties. In *IGARSS'03, Proceedings of the International Geoscience and Remote Sensing Symposium*, 24–28 July 2003, Toulouse, France. IEEE, New York.
- Lee, J.S., Grues, M.R., Pottier, E., and Ferro-Famil, L. 2004. Unsupervised terrain classification preserving scattering characteristics. *IEEE Transactions on Geoscience and Remote Sensing*. In press.
- Lewinski, D.J. 1983. Nonstationary probabilistic target and clutter scattering models. *IEEE Transactions on Antennas and Propagation*, Vol. 31, pp. 490–498.
- Lim, H.H., Swartz, A.A., Kong, J.A., Shin, R.T., and Van Zyl, J.J. 1989. Classification of earth terrain using polarimetric synthetic aperture radar images. *Journal of Geophysical Research*, Vol. 94, pp. 7049–7057.
- Livingstone, C.E., Lukowski, T.I., Rey, M.T., Lafontaine, J.R.C., and Campbell, J.W. 1989. CCRS/DREO synthetic aperture radar polarimetry — status report. In *IGARSS'89, Proceedings of the International Geoscience and Remote Sensing Symposium*, 10–14 July 1989, Vancouver, B.C. IEEE, New York.
- Livingstone, C.E., Gray, A.L., Hawkins, R.K., Vachon, P.W., Lukowski, T.I., and LaLonde, M. 1995. The CCRS airborne SAR systems: radar for remote sensing research. *Canadian Journal of Remote Sensing*, Vol. 21, No. 4, pp. 468–491.
- Lombardo, P., and Oliver, C.J. 2002. Optimum polarimetric segmentation for the classification of agricultural areas. In *EUSAR 2002, Proceedings of the 4th European Union Conference on Synthetic Aperture Radar*, 4–6 June 2002, Cologne, Germany.
- Lopes, A., and Sery, F. 1997. Optimal speckle reduction for the product model in multilook polarimetric SAR imagery and the Wishart distribution. *IEEE Transactions on Geoscience and Remote Sensing*, Vol. 35, pp. 632–647.
- Lopes, A., Mougin, R.E., Baudoïn, A., Goze, S., Nezry, E., Touzi, R., and Karam, M. 1992. Phase difference statistics related to sensor and forest parameters. In *IGARSS'92, Proceedings of the International Geoscience and Remote Sensing Symposium*, 26–29 May 1992, Houston, Tex. IEEE, New York. pp. 779–781.
- Lüneburg, E. 1995a. Principles of radar polarimetry — using the directional Jones vector approach. *IEICE Transactions on Electronics (Special Issue on Electromagnetic Theory)*, Vol. E78-C, No. 10, pp. 1339–1345.
- Lüneburg, E. 1995b. Canonical bases and Huynen decomposition. In *Proceedings of the 3rd International Workshop on Radar Polarimetry (JIPR)*, 21–23 Mar. 1995, IRESTE, University of Nantes, Nantes, France. pp. 75–83.
- Lüneburg, E. 2002. Aspects of radar polarimetry. *Elektrik-Turkish Journal of Electrical Engineering and Computer Sciences*, Vol. 10, No. 2, pp. 219–243.
- Luscombe, A.P., Chotoo, K., and Huxtable, B.D. 2000. Polarimetric calibration of RADARSAT 2. In *IGARSS'00, Proceedings of the International Geoscience and Remote Sensing Symposium*, 24–28 July 2000, Honolulu, Hawaii. IEEE, New York.
- Mandel, L. 1963. Intensity fluctuations of partially polarized light. *Proceedings of the Physical Society*, Vol. 81, pp. 1104–1114.
- Mandel, L., and Wolf, E. 1995. *Optical coherence and quantum optics*. Cambridge University Press, Cambridge, Mass. 1192 pp.

- Mathew, C.H. 2001. Design and development of a European space-borne L-band SAR. In *Proceedings of the CEOS SAR Workshop 2001*, 2–5 April 2001, Tokyo, Japan. National Space Development Agency of Japan (NASDA), Tokyo.
- Mattia, F., Le Toan, T., Souyris, J.C., De Carolis, G., Floury, N., Posa, F., and Pasquariello, G. 1997. The effect of surface roughness on multi-frequency polarimetric SAR data. *IEEE Transactions on Geoscience and Remote Sensing*, Vol. 35, No. 4, pp. 954–966.
- McConnell, I., White, R., Oliver, C., and Cook, R. 1995. Radar cross-section estimation of SAR images. In *Laser techniques for state-selected and state-to-state chemistry*. Edited by J.W. Hepburn. International Society for Optical Engineering, Bellingham, Wash. Proceedings of SPIE, Vol. 2548, pp. 164–175.
- McCormick, G.C. 1996. The theory of polarization diversity systems: the partially polarized case. *IEEE Transactions on Antennas and Propagation*, Vol. AP-44, No. 1, pp. 425–433.
- McCormick, G.C., and Hendry, A. 1973. Method of measuring the anisotropy of precipitation media. *Electronic Letters*, Vol. 9, pp. 216–218.
- McCormick, G.C., and Hendry, A. 1985. Optimum polarizations for partially polarized backscatter. *IEEE Transactions on Antennas and Propagation*, Vol. AP-33, No. 1, pp. 33–39.
- McNairn, H., Duguay, C., Brisco, B., and Pultz, T.J. 2002. The effect of soil and crop residue characteristics on polarimetric radar response. *Remote Sensing of Environment*, Vol. 80, No. 2, pp. 308–320.
- Mott, H. 1992. *Antennas for radar and communications, a polarimetric approach*. John Wiley & Sons, Inc., New York. 521 pp.
- Mueller, H. 1948. The foundations of optics. *Journal of the Optical Society of America*, Vol. 38, pp. 661–662.
- Murza, L.P. 1978. The noncoherent polarimetry of noise like radiation. *Radio Engineering and Electronic Physics*, Vol. 23, pp. 57–63.
- Novak, L.M., and Burl, M.C. 1990. Optimal speckle reduction in polarimetric SAR imagery. *IEEE Transactions on Aerospace and Electronic Systems*, Vol. 26, pp. 293–305.
- Oliver, C., and Quegan, S. 1998. *Understanding synthetic aperture radar images*. Artech House, Norwood, Mass.
- Papathanassiou, K.P., and Cloude, S.R. 2001. Single baseline polarimetric SAR interferometry. *IEEE Transactions on Geoscience and Remote Sensing*, Vol. 39, No. 11, pp. 2352–2363.
- Papathanassiou, K.P., and Cloude, S.R. 2003. The effect of temporal decorrelation on the inversion of forest parameters from Pol-InSAR data. In *IGARSS'03, Proceedings of the International Geoscience and Remote Sensing Symposium*, 24–28 July 2003, Toulouse, France. IEEE, New York.
- Parrent, G.B., and Roman, P. 1960. On the matrix formulation of the theory of partial polarization in terms of observables. *Nuovo Cimento*, Vol. 15, No. 3, pp. 370–387.
- Poelman, A.J., and Guy, J.R.F. 1984. Multinoch logic-product polarization suppression filters. *Proceedings of Institution of Electrical Engineers*, Vol. 130, No. 4, pp. 383–396.
- Poincaré, H. 1892. *Théorie mathématique de la lumière*. Georges Carre, Paris, France.
- Pottier, E., and Cloude, S.R. 1995. Unsupervised classification of full polarimetric SAR data using target decomposition theorem and entropy analysis. In *IGARSS'95, Proceedings of the International Geoscience and Remote Sensing Symposium*, 10–14 July 1995, Florence, Italy. IEEE, New York. pp. 2247–2249.
- Pottier, E., and Lee, J.S. 1999. Application of the H/A/α polarimetric decomposition theorem for unsupervised classification of fully polarimetric SAR data based on the Wishart distribution. In *Proceedings of the CEOS'99 Workshop*, 26–29 Oct. 1999, Toulouse, France. ESA Publications Division, Noordwijk, The Netherlands, ESA SP-450. Available from <http://www.estec.esa.nl/CONFANNOUN/99b02>.
- Pottier, E., Lee, J.-S., Ainsworth, T.A., Schuler, D.L., and Boerner, W.-M. 1999. Compensation for terrain azimuthal slope variation. *IEEE Transactions on Geoscience and Remote Sensing*, Vol. 37, No. 6.
- Quegan, S. 1993. A unified algorithm for phase and cross-talk calibration of polarimetric data. *IEEE Transactions on Geoscience and Remote Sensing*, Vol. 2, pp. 9–99.
- Quegan, S., and Rhodes, I. 1995. Statistical models for polarimetric data: consequences, testing and validity. *International Journal of Remote Sensing*, Vol. 16, No. 7, pp. 1183–1210.
- Rais, H., and Mansfield, A.W. 1999. L-band/P-band SAR comparison for search and rescue: recent results. In *Proceedings of the SPIE Aerosense Conference*, 5–9 April 1999, Orlando, Fla. International Society for Optical Engineering, Bellingham, Wash.
- Raney, R.K. 1980. SAR response to partially coherent phenomena. *IEEE Transactions on Antennas Propagation*, Vol. AP-26, pp. 777–787.
- Raney, R.K. 1998. Radar fundamentals: technical perspective. In *Manual of remote sensing*. Edited by R.A. Ryerson. John Wiley and Sons, Inc., New York. Principles and Applications of Imaging Radar, Vol. 3, No. 5, pp. 9–130.
- Rignot, E. 2000. Effect of Faraday rotation on L-band interferometric and polarimetric synthetic aperture radar data. *IEEE Transactions on Geoscience and Remote Sensing*, Vol. 38, No. 1, pp. 383–390.
- Rignot, E., Chellapa, R., and Dubois, P. 1992. Unsupervised segmentation of polarimetric SAR data using the covariance matrix. *IEEE Transactions on Geoscience and Remote Sensing*, Vol. 30, No. 4, pp. 697–705.
- Rumsey, V.H. 1951. Transmission between elliptically polarized antennas. *Proceedings of the IRE*, Vol. 39, pp. 535–540.
- Saleh, B.E.A., and Rabbani, M. 1980. Linear filtering of speckled images. *Optics Communications*, Vol. 35, pp. 327–331.
- Sarabandi, K. 1992. Derivation of phase statistics from the Mueller matrix. *Radio Science*, Vol. 27, pp. 553–560.
- Sarabandi, K., Pierce, L.K., Dobson, M.C., Ulaby, F.T., Stiles, J., Chin, T.C., DeRoo, R., Hartikka, R., Zambetti, A., and Freeman, A. 1995. Polarimetric calibration of SIR-C using point and distributed targets. *IEEE Transactions on Antennas and Propagation*, Vol. AP-33, No. 4, pp. 858–866.
- Scheiber, R., Reigber, A., Papathanassiou, K.P., Horn, R., Buckreuz, S., and Moreira, A. 1999. Overview of interferometric data acquisition and processing modes of the experimental airborne SAR system of DLR. In *IGARSS'99, Proceedings of the International Geoscience and Remote Sensing Symposium*, June 1999, Hamburg, Germany. IEEE, New York.
- Scheuchl, B., Cumming, I., and Hajnsek, I. 2003. Classification of ice type from Convair-580 SAR data of Northumberland Strait, PEI. In *ASAR/CEOS'2003, Proceedings of the Advanced SAR Workshop*, 24–27 June 2003, Montréal, Que. Canadian Space Agency, St. Hubert, Que.
- Schneider, R. 1969. Stokes algebra formalism. *Journal of the Optical Society of America*, Vol. 59, pp. 297–302.

- Schou, J., and Skriver, H. 2001. Restoration of polarimetric SAR images using simulated annealing. *IEEE Transactions on Geoscience and Remote Sensing*, Vol. 39, No. 9, pp. 2005–2016.
- Schou, J., Skriver, H., Nielsen, A.A., and Conradsen, K. 2003. CFAR edge detector for polarimetric SAR images. *IEEE Transactions on Geoscience and Remote Sensing*, Vol. 41, No. 1, pp. 20–32.
- Schuler, D.L., Lee, J.S., and De Grandi, G. 1996. Measurement of topography using polarimetric SAR images. *IEEE Transactions on Geoscience and Remote Sensing*, Vol. 34, No. 5, pp. 1210–1221.
- Schuler, D.L., Lee, J.S., Ainsworth, T.L., and Grues, M.R. 2000. Terrain topography measurement using multipass polarimetric synthetic aperture radar data. *Radio Science*, Vol. 35, No. 3, pp. 813–832.
- Schuler, D.L., Lee, J.S., and Kasilingam, D. 2002. Surface roughness and slope measurements using polarimetric SAR data. *IEEE Transactions on Geoscience and Remote Sensing*, Vol. 40, No. 3, pp. 687–698.
- Schwerdt, M., Hounam, D., Molkenthin, T., and Alvarez-Peres, J.L. 2003. Calibration concepts for multiple mode high resolution SARs like TerraSAR-X. In *ASAR/CEOS'2003, Proceedings of the Advanced SAR Workshop*, 24–27 June 2003, Montréal, Que. Canadian Space Agency, St. Hubert, Que.
- Sheen, D.R., and Johnson, L.P. 1992. Statistical and spatial properties of forest clutter measured with polarimetric synthetic aperture radar. *IEEE Transactions on Geoscience and Remote Sensing*, Vol. 30, pp. 578–588.
- Shimada, M. 2001. Calibration and validation of PALSAR and research products of NASDA/EORC. In *Proceedings of the CEOS SAR Workshop 2001*, 2–5 April 2001, Tokyo, Japan. National Space Development Agency of Japan (NASDA), Tokyo.
- Simon, R. 1982. The connection between Mueller and Jones matrices of polarization optics. *Optics Communications*, Vol. 42, pp. 293–297.
- Sinclair, G. 1950. Transmission and reception of elliptically polarized waves. *Proceedings of the IRE*, Vol. 38, pp. 148–151.
- Skou, N., Granholm, J., Woelders, K., Rohde, J., Dall, J., and Christensen, E.L. 1995. A high resolution polarimetric L-band SAR — design and first results. In *IGARSS'85, Proceedings of the International Geoscience and Remote Sensing Symposium*, 7–9 Oct. 1985, Amherst, Mass. IEEE, New York. pp. 1779–1782.
- Skriver, H., Dall, J., and Madsen, S.N. 1994. External polarimetric calibration of the Danish polarimetric C-band SAR. In *IGARSS'94, Proceedings of the International Geoscience and Remote Sensing Symposium*, 8–12 Aug. 1994, Pasadena, Calif. IEEE, New York. pp. 1105–1107.
- Souyris, J.C., Henry, C., and Adragana, F. 2004. On the use of complex SAR image spectral analysis for target detection: assessment of polarimetry. *IEEE Transactions on Geoscience and Remote Sensing*. In press.
- Stokes, G.G. 1852. On the composition and resolution of streams of polarized light from different sources. *Transactions of the Cambridge Philosophical Society*, Vol. 9, pp. 399–416.
- Swartz, A.A., Yueh, H.A., Kong, J.A., Novak, L.M., and Shin, R.T. 1988. Optimal polarizations for archiving maximum contrast in radar images. *Journal of Geophysical Research*, Vol. 93, pp. 15 252 – 15 260.
- Takagi, T. 1927. On an algebraic problem related to an analytical theorem of Caratheodory and Fejer and on an allied theorem of Landau. *Japanese Journal of Mathematics*, Vol. 1, pp. 83–93.
- Touzi, R. 1992. Extraction of point target response characteristics from complex SAR data. *IEEE Transactions on Geoscience and Remote Sensing*, Vol. 30, pp. 1158–1161.
- Touzi, R. 1999a. Calibration and analysis of Convair-580 polarimetric SAR data for forest target characterization. Canada Centre for Remote Sensing, Ottawa, Ont. Technical Report to the Defense Research Establishment of Ottawa (DREO) under the CCRS/DREO agreement FY97/98-98/99.
- Touzi, R. 1999b. On the use of polarimetric SAR data for ship detection. In *IGARSS'99, Proceedings of the International Geoscience and Remote Sensing Symposium*, June 1999, Hamburg, Germany. IEEE, New York.
- Touzi, R. 2000. Calibrated polarimetric SAR data for ship detection. In *IGARSS'00, Proceedings of the International Geoscience and Remote Sensing Symposium*, 24–28 July 2000, Honolulu, Hawaii. IEEE, New York.
- Touzi, R. 2002. A review of SAR image speckle filtering. *IEEE Transactions on Geoscience and Remote Sensing*, Vol. 40, pp. 2392–2404.
- Touzi, R., and Charbonneau, F. 2002. Characterization of target symmetric scattering using polarimetric SARs. *IEEE Transactions on Geoscience and Remote Sensing*, Vol. 40, pp. 2507–2516.
- Touzi, R., and Charbonneau, F. 2003. Ship characterization using polarimetric SARs. In *IGARSS'03, Proceedings of the International Geoscience and Remote Sensing Symposium*, 24–28 July 2003, Toulouse, France. IEEE, New York.
- Touzi, R., and Livingstone, C.E. 2003. A general method for the calibration of the C-band Convair-580 polarimetric SAR. In *ASAR/CEOS'2003, Proceedings of the Advanced SAR Workshop*, 24–27 June 2003, Montréal, Que. Canadian Space Agency, St. Hubert, Que.
- Touzi, R., and Lopes, A. 1991. Distribution of the Stokes parameters and the phase difference in polarimetric SAR data. In *IGARSS'91, Proceedings of the International Geoscience and Remote Sensing Symposium*, 3–6 June 1991, Espoo, Finland. IEEE, New York.
- Touzi, R., and Lopes, A. 1994. The principle of speckle filtering in polarimetric SAR imagery. *IEEE Transactions on Geoscience and Remote Sensing*, Vol. 32, pp. 1110–1114.
- Touzi, R., and Lopes, A. 1996. Statistics of the Stokes parameters and of the complex coherence parameters in one-look and multi-look speckle fields. *IEEE Transactions on Geoscience and Remote Sensing*, Vol. 34, pp. 519–531.
- Touzi, R., Goze, S., Le Toan, T., Lopes, A., and Mougin, E. 1992a. Polarimetric discriminators for SAR images. *IEEE Transactions on Geoscience and Remote Sensing*, Vol. 30, No. 5, pp. 973–980.
- Touzi, R., Raney, R.K., and Lopes, A. 1992b. On the use of SAR complex data for calibration. In *IGARSS'92, Proceedings of the International Geoscience and Remote Sensing Symposium*, 26–29 May 1992, Houston, Tex. IEEE, New York. pp. 1155–1157.
- Touzi, R., Livingstone, C.E., Lafontaine, J.R.C., and Lukowski, T.I. 1993. Consideration of antenna gain and phase patterns for calibration of polarimetric SAR data. *IEEE Transactions on Geoscience and Remote Sensing*, Vol. 31, No. 6, pp. 1132–1145.
- Touzi, R., Lopes, A., Bruniquel, J., and Vachon, P.W. 1999. Coherence estimation for SAR imagery. *IEEE Transactions on Geoscience and Remote Sensing*, Vol. 37, pp. 135–149.
- Touzi, R., Freeman, A., Dubois, P., Boerner, W., Pottier, E., and Mercier, B. 2003. Session summary: polarimetric–interferometric processing and application. In *ASAR/CEOS'2003, Proceedings of the Advanced SAR*

- Workshop, 24–27 June 2003, Montréal, Que. Canadian Space Agency, St. Hubert, Que.
- Touzi, R., Charbonneau, F.J., Hawkins, R.K., and Vachon, P.W. 2004a. Ship detection and characterization using polarimetric SAR. *Canadian Journal of Remote Sensing*, Vol. 30, No. 3, pp. 552–559.
- Touzi, R., Landry, R., and Charbonneau, F.J. 2004b. Forest type discrimination using calibrated C-band polarimetric SAR data. *Canadian Journal of Remote Sensing*, Vol. 30, No. 3, pp. 543–551.
- Touzi, R., Raney, R.K., and Charbonneau, F. 2004c. On the use of symmetric scatterers for ship characterization. *IEEE Transactions on Geoscience and Remote Sensing*. In press.
- Tragl, K. 1990. Polarimetric radar backscatter from reciprocal random targets. *IEEE Transactions on Geoscience and Remote Sensing*, Vol. 28, pp. 856–864.
- Treuhaft, R.N., and Siqueira, P.R. 2000. Vertical structure of vegetated land surfaces from interferometric and polarimetric data. *Radio Science*, Vol. 35, pp. 141–177.
- Treuhaft, R.N., Madsen, S.N., Moghaddam, M., and Van Zyl, J.J. 1996. Vegetation characteristics and surface topography from interferometric radar. *Radio Science*, Vol. 31, pp. 1449–1485.
- Tsang, L., Kong, J.A., and Shin, R.T. 1985. *Theory of microwave remote sensing*. Wiley Interscience, New York.
- Tur, M., Chin, K.C., and Goodman, J.W. 1982. When is speckle multiplicative? *Applied Optics*, Vol. 21, pp. 1157–1159.
- Ulaby, F.T., and Elachi, C. 1990. *Radar polarimetry for geoscience applications*. Artech House, Norwood, Mass.
- Vachula, G.M., and Barnes, R.M. 1983. Polarization detection of a fluctuating radar target. *IEEE Transactions on Aerospace and Electronic Systems*, Vol. AES-19, No. 2, pp. 250–257.
- Van de Hulst, H.C. 1957. *Light scattering by small particles*. Wiley, New York.
- Van Zyl, J.J. 1989. Unsupervised classification of scattering behavior using radar polarimetry data. *IEEE Transactions on Geoscience and Remote Sensing*, Vol. 27, No. 1, pp. 37–45.
- Van Zyl, J.J. 1990. Calibration of polarimetric radar images using only image parameters and trihedral corner reflectors responses. *IEEE Transactions on Geoscience and Remote Sensing*, Vol. 28, No. 3, pp. 337–348.
- Van Zyl, J.J. 1992. Application of Cloude's target decomposition theorem to polarimetric imaging radar data. In *Radar polarimetry*. Edited by H. Mott and W.M. Boerner. International Society for Optical Engineering, Bellingham, Wash. Proceedings of SPIE, Vol. 1748, pp. 184–191.
- Van Zyl, J.J., and Ulaby, F.T. 1990. Scattering matrix representation for simple targets. In *Radar polarimetry for geoscience applications*. Edited by F.T. Ulaby and C. Elachi. Artech House, Norwood, Mass. Chapt. 2, pp. 17–50.
- Van Zyl, J.J., and Zebker, H.A. 1990. Imaging radar polarimetry. In *Polarimetric remote sensing*. Edited by J.A. Kong. Elsevier, New York. Progress in Electromagnetics Research (PIER), Vol. 3, Chapt. 5.
- Van Zyl, J.J., Zebker, H.A., and Elachi, C. 1987a. Imaging radar polarization signatures: theory and observation. *Radio Science*, Vol. 22, pp. 529–543.
- Van Zyl, J.J., Papas, C.H., and Elachi, C. 1987b. On the optimum polarizations of incoherently reflected waves. *IEEE Transactions on Antennas and Propagation*, Vol. AP-35, No. 7, pp. 818–825.
- Van Zyl, J.J., Chapman, B.D., Dubois, P., and Freeman, A. 1992. *POLCAL user's manual*. Jet Propulsion Laboratory, Pasadena, Calif. Technical Report, JPL Document D-7715.
- Van Zyl, J.J., Chapman, B.D., and Dubois, P.T. 1993. The effect of topography on SAR calibration. *IEEE Transactions on Geoscience and Remote Sensing*, Vol. 31, No. 5, pp. 1036–1043.
- Von Neumann, J. 1955. *Mathematical foundation of quantum mechanics*. Princeton University Press, Princeton, N.J.
- Wakabayashi, H., Tadono, T., and Matsuoka, M. 2001. Cross-calibration of airborne L-band polarimetric SAR. In *Proceedings of the CEOS SAR Workshop 2001*, 2–5 April 2001, Tokyo, Japan. National Space Development Agency of Japan (NASDA), Tokyo.
- Wiener, N. 1930. Generalized harmonic analysis. *Acta Mathematica*, Vol. 5, pp. 118–258.
- Wishart, J. 1928. The generalized product moment distribution in samples from a normal multivariate population. *Biometrika*, Vol. 20A, pp. 32–52.
- Wolf, E. 1954. Optics in terms of observable quantities. *Nuovo Cimento*, Vol. 12, pp. 884–888.
- Wolf, E. 1959. Coherence properties of partially polarized electromagnetic radiation. *Nuovo Cimento*, Vol. 13, No. 6, pp. 1165–1181.
- Wright, P., Quegan, S., Wheadon, N., and Hall, D. 2003. Faraday rotation effects on L-band spaceborne SAR data. *IEEE Transactions on Geoscience and Remote Sensing*, Vol. 41, No. 12, pp. 2735–2744.
- Jeremy, M., Campbell, J.W.M., Mattar, K., and Potter, T. 2001. Ocean surveillance with polarimetric SAR. *Canadian Journal of Remote Sensing*, Vol. 27, No. 4, pp. 328–344.
- Yueh, S.H., Kong, J.A., Jao, J.K., Shin, R.T., and Novak, L.M. 1989. K distribution and terrain radar clutter. *Journal of Electromagnetic Waves and Applications*, Vol. 3, No. 8, pp. 747–768.
- Yueh, S.H., Kong, J.A., Jao, J.K., Shin, R.T., Novak, L.M., and Le Toan, T. 1991. K distribution and multi-frequency polarimetric terrain radar clutter. *Journal of Electromagnetic Waves and Applications*, Vol. 5, No. 1, pp. 1–15.
- Zebker, H.A., and Lou, Y. 1990. Phase calibration of imaging radar polarimeter stokes matrices. *IEEE Transactions on Geoscience and Remote Sensing*, Vol. 28, No. 2, pp. 246–252.
- Zebker, F.A., and Van Zyl, J.J. 1991. Imaging radar polarimetry: a review. *Proceedings of the IEEE*, Vol. 79, pp. 1583–1606.
- Zebker, H.A., Van Zyl, J.J., and Held, D.N. 1987. Imaging radar polarimetry from wave synthesis. *Journal of Geophysical Research*, Vol. 92, pp. 683–701.